



Deposited via The University of Leeds.

White Rose Research Online URL for this paper:

<https://eprints.whiterose.ac.uk/id/eprint/151669/>

Version: Accepted Version

Article:

Suprisunjai, C, Hsu, C-K, Michael, M et al. (2020) Coagulation Factor XIII-A Subunit Missense Mutation in the Pathobiology of Autosomal Dominant Multiple Dermatofibromas. *The Journal of Investigative Dermatology*, 140 (3). pp. 624-635. ISSN: 0022-202X

<https://doi.org/10.1016/j.jid.2019.08.441>

(c) 2019, The Authors. Published by Elsevier, Inc. on behalf of the Society for Investigative Dermatology. This manuscript version is made available under the CC-BY-NC-ND 4.0 license <https://creativecommons.org/licenses/by-nc-nd/4.0/>

Reuse

This article is distributed under the terms of the Creative Commons Attribution-NonCommercial-NoDerivs (CC BY-NC-ND) licence. This licence only allows you to download this work and share it with others as long as you credit the authors, but you can't change the article in any way or use it commercially. More information and the full terms of the licence here: <https://creativecommons.org/licenses/>

Takedown

If you consider content in White Rose Research Online to be in breach of UK law, please notify us by emailing eprints@whiterose.ac.uk including the URL of the record and the reason for the withdrawal request.

JID-2019-0484.R1**Coagulation Factor XIII-A Subunit Missense Mutation in the Pathobiology of Autosomal Dominant Multiple Dermatofibromas**

Chavalit Supsrirunjai^{1,2}, Chao-Kai Hsu^{1,3,4}, Magdalene Michael⁵, Cédric Duval⁶, John Y. W. Lee¹, Hsing-San Yang³, Hsin-Yu Huang⁷, Thitiwat Chaikul¹, Alexandros Onoufriadis¹, Roberto A. Steiner⁵, Robert A. S. Ariëns⁶, Ofer Sarig⁸, Eli Sprecher^{8,9}, Marina Schwartz-Eskin⁸, Curt Samlaska¹⁰, Michael A. Simpson¹¹, Eduardo Calonje^{1,12}, Maddy Parsons^{5*}, John A. McGrath^{1*}

ORCIDs

Chavalit Supsrirunjai: <https://orcid.org/0000-0002-1054-6918>

Chao-Kai Hsu: <https://orcid.org/0000-0003-4365-4533>

Magdalene Michael: <https://orcid.org/0000-0003-2577-729X>

Cédric Duval: <https://orcid.org/0000-0002-4870-6542>

John Y. W. Lee: <https://orcid.org/0000-0002-5563-2334>

Hsing-San Yang: <https://orcid.org/0000-0002-3973-2896>

Hsin-Yu Huang: <https://orcid.org/0000-0003-0220-3509>

Thitiwat Chaikul: <https://orcid.org/0000-0001-5463-3864>

Alexandros Onoufriadis: <https://orcid.org/0000-0001-5026-0431>

Roberto Steiner: <https://orcid.org/0000-0001-7084-9745>

Robert A. S. Ariëns: <https://orcid.org/0000-0002-6310-5745>

Ofer Sarig: <https://orcid.org/0000-0003-2987-2091>

Eli Sprecher: <https://orcid.org/0000-0003-0666-0045>

1
2
3 Marina Schwartz-Eskin: <https://orcid.org/0000-0003-0507-1505>
4

5 Curt Samlaska: <https://orcid.org/0000-0001-7562-4254>
6

7 Michael A. Simpson: <https://orcid.org/0000-0002-8539-8753>
8

9 Eduardo Calonje : <https://orcid.org/0000-0001-7475-6423>
10

11 Maddy Parsons: <https://orcid.org/0000-0002-2021-8379>
12

13 John A. McGrath: <https://orcid.org/0000-0002-3708-9964>
14
15
16
17

18 ¹St John's Institute of Dermatology, School of Basic and Medical Biosciences, King's College
19 London, Guy's Hospital, London, UK
20

21 ²Institute of Dermatology, Ministry of Public Health, Bangkok, Thailand
22

23 ³Department of Dermatology, National Cheng Kung University Hospital, College of Medicine,
24 National Cheng Kung University, Tainan, Taiwan
25

26 ⁴International Center for Wound Repair and Regeneration, National Cheng Kung University,
27 Tainan, Taiwan
28

29 ⁵Randall Centre for Cell and Molecular Biophysics, School of Basic and Medical Biosciences,
30 King's College London, UK
31

32 ⁶Leeds Institute of Cardiovascular and Metabolic Medicine, University of Leeds, Leeds, UK
33

34 ⁷School of Medicine, College of Medicine, National Cheng Kung University, Tainan, Taiwan
35

36 ⁸Division of Dermatology, Tel Aviv Sourasky Medical Center, Tel Aviv, Israel
37

38 ⁹Department of Human Molecular Genetics & Biochemistry, Sackler Faculty of
39 Medicine, Tel-Aviv University, Tel-Aviv, Israel
40

41 ¹⁰Academic Dermatology of Nevada, University of Nevada School of Medicine, Reno, Nevada
42

43 ¹¹Department of Genetics, School of Basic and Medical Biosciences, King's College London,
44 Guy's Hospital, London, UK
45
46
47
48
49
50
51
52
53
54
55
56
57
58
59
60

1
2
3 ¹²Department of Dermatopathology, St John's Institute of Dermatology, Guy's and St Thomas'
4 NHS Foundation Trust, London SE1 9RT, UK
5
6
7
8
9

10 * Joint senior authors. Correspondence should be addressed to JAM (john.mcgrath@kcl.ac.uk)
11
12
13
14
15

16 **Corresponding author:** John McGrath, Dermatology Research Labs, Floor 9 Tower Wing,
17 Guy's Hospital, Great Maze Pond, London SE1 9RT, United Kingdom. Tel: 44-2071886409;
18 Fax: 44-2071888050; E-mail: john.mcgrath@kcl.ac.uk
19
20
21
22
23
24
25

26 **Short title:** *F13A1* mutation causes familial dermatofibroma
27
28

29 **Abbreviations used:**
30
31

32 Å angstrom
33
34

35 Akt acutely transforming retrovirus AKT8 in rodent T cell lymphoma
36
37

38 CDM cell-derived matrix
39
40

41 Col I collagen type I
42
43

44 ERK extracellular signal-regulated kinase
45
46

47 ExAC Exome Aggregation Consortium
48
49

50 FBS fetal bovine serum
51
52

53 FN fibronectin
54
55

56 FXIII-A Factor XIII subunit A
57
58

59 GAPDH glyceraldehyde-3-phosphate dehydrogenase
60

1
2
3 GFP green fluorescent protein
4
5
6 GST glutathione S-Transferase
7
8
9 GTP guanosine triphosphate
10
11
12 HEK human embryonic kidney
13
14
15 HET heterozygous
16
17
18 HRP horseradish peroxidase
19
20
21 ILDT Isoleucine-Leucine-Aspartate-Threonine
22
23
24 IRES internal ribosome entry site
25
26
27 MAPK mitogen-activated protein kinase
28
29
30 NHDF normal human dermal fibroblast
31
32
33 PBS phosphate buffered saline
34
35
36 PDGF platelet-derived growth factor
37
38
39 PDGFR platelet-derived growth factor receptor
40
41
42 PI3K phosphatidylinositol 3 kinase
43
44
45 TBS Tris buffered saline
46
47
48 WES whole exome sequencing
49
50
51 WT wild type
52
53
54
55
56
57
58
59
60

Abstract

Dermatofibromas are common benign skin lesions, the etiology of which is poorly understood. We identified two unrelated pedigrees in which there was autosomal dominant transmission of multiple dermatofibromas. Whole exome sequencing revealed a rare shared heterozygous missense variant in *F13A1* gene encoding factor XIII subunit A, a transglutaminase involved in hemostasis, wound healing, tumor growth, and apoptosis. The variant (p.Lys679Met) has an allele frequency of 0.0002 and is predicted to be a damaging mutation. Recombinant human Lys679Met FXIII-A demonstrated reduced fibrin crosslinking activity *in vitro*. Of note, treatment of fibroblasts with media containing Lys679Met FXIII-A led to enhanced adhesion, proliferation and type I collagen synthesis. Immunostaining revealed co-localization between FXIII-A and $\alpha4\beta1$ integrins, more prominently for Lys679Met FXIII-A than wild-type. In addition, both the $\alpha4\beta1$ inhibitors and the mutation of the FXIII-A Isoleucine-Leucine-Aspartate-Threonine (ILDT) motif prevented Lys679Met FXIII-A-dependent proliferation and collagen synthesis of fibroblasts. Our data suggest that the Lys679Met mutation may leads to a conformational change in the FXIII-A protein that enhances $\alpha4$ -integrin binding and provide insight into an unexpected role for FXIII-A in the pathobiology of familial dermatofibroma.

INTRODUCTION

Dermatofibromas are common benign fibro-histiocytic tumors (Jakobiec et al., 2014; 2017).
Typically, dermatofibromas present as solitary 0.5-1cm pink, red, tan or flesh-colored lumps
with an overlying dimple-like depression (Zelger and Zelger, 1998). Sometimes multiple
dermatofibromas may occur, occasionally in families, but more often in individuals with
underlying immunologic or other clinical abnormalities (Beatrous et al., 2017). The most
common site for dermatofibromas is the lower legs, with usual onset during early adulthood.
The cause of dermatofibromas is not known although dermatologists may suggest they occur
following insect bites in susceptible individuals, or possibly following trauma (Kluger et al.,
2008; Myers and Fillman 2019).

Histologically, in dermatofibromas (single or multiple) there are interlacing fascicles
of slender spindle-shaped cells within a loose collagenous, or occasionally myxoid, stroma. Of
note, hemosiderin is frequently present. Immunohistochemically, almost all dermatofibromas
are FXIII-A (factor XIIIa antigen)-positive (Altman et al., 1993), and indeed immunostaining
for FXIII-A is frequently used in the tissue diagnosis of dermatofibromas (Cerio et al., 1988;
1989).

In this study, we performed whole exome sequencing (WES) to identify the causative
mutation in two seemingly unrelated pedigrees with autosomal dominant familial multiple
dermatofibromas. Intriguingly, we identified the same mutation in *FXIII-A* encoding the A-
subunit of factor XIII (FXIII-A) in both families. FXIII is a member of transglutaminase family
which crosslinks various proteins involved in hemostasis, wound healing, tumor growth, and
apoptosis (Muszbek et al., 2011). During wound healing, FXIII modulates fibroblast and
macrophage biology and contributes to angiogenesis (Bagoly et al., 2012, Duval et al., 2016,
Muszbek et al., 2011). While plasma FXIII is composed of two catalytic A subunits and two

1
2
3 non-catalytic carrier B units generating a A₂B₂ heterotetramer (Komaromi et al., 2011), cellular
4
5 FXIII (found, for example, in platelets and megakaryocytes) is formed solely of A subunits
6
7 organized in an A₂ homodimer. The mutation we identified in this study affects the A subunit,
8
9 i.e. it impacts on both the plasma and tissue/cellular FXIII forms (PMID: 30489000, PMID:
10
11 5096097). We provide evidence that the FXIII-A mutation leads to enhanced proliferation and
12
13 collagen synthesis in fibroblasts, potentially through promoting binding of exogenous FXIII-
14
15 A to integrins. Our study therefore provides insight into an important role for FXIII-A in the
16
17 etiology and pathobiology of some dermatofibromas.
18
19
20
21
22
23
24

25 RESULTS

31 Clinical features and histology

32
33 We examined seven affected individuals from two unrelated families with multiple
34
35 dermatofibromas inherited in an autosomal dominant pattern (Figure 1a). Three affected
36
37 individuals were from the Ukraine (Family 1) and four affected were from the USA (Family
38
39 2). Both families were Jewish (Ashkenazi). Some clinicopathologic details of Family 2 have
40
41 been published previously (Samlaska and Bennion, 2002). All subjects presented with multiple
42
43 lesions of erythematous papules over extremities (Figure 1b; illustrations from Family 1 and
44
45 2) with histopathologic findings of dermatofibromas (Figure 1c; Family 1, II-2). No extra-
46
47 cutaneous manifestations were reported.
48
49
50
51
52
53
54
55

56 **All individuals with multiple dermatofibromas are heterozygous for the mutation**
57
58 **c.2036A>T (Lys679Met) in *F13A1***
59
60

1
2
3 We undertook WES in six affected subjects from the Ukraine and US families and two
4 unaffected individuals from the US family. Candidate mutations were prioritized by filtering
5 for variants with a frequency of less than 0.01% in public repositories such as the 1000
6 Genomes Project, Exome Aggregation Consortium (ExAC) and an in-house database
7 (Supplementary Table S1, S2). Using these criteria, a missense variant in *F13A1* encoding
8 Factor XIII subunit A (c.2036A>T; rs201302247) was the only variant present in all affected
9 individuals in both families. Subsequent Sanger sequencing confirmed the mutation in affected
10 individuals (Supplementary Figure S1) and co-segregated with disease status in all relatives
11 who provided DNA samples. This variant was rare in the population (less than 0.0207%
12 frequency) and resulted in an amino acid change from lysine to methionine at position 679
13 (position 678 in the mature protein) with an *in silico* prediction that the mutation is damaging
14 (Polyphen-2 = 1; Mutation taster = 1; CADD = 25.5; DANN = 0.993).
15
16
17
18
19
20
21
22
23
24
25
26
27
28
29
30
31
32
33

c.2036A>T in *F13A1* is a rare allele found most commonly in Ashkenazi Jews

34
35
36
37 To investigate the possibility that c.2036A>T was inherited from a common ancestor, we
38 performed a haplotype analysis to study the mutant alleles from affected individuals using four
39 highly polymorphic single nucleotides polymorphism markers based on the exome data
40 (Supplementary Figure S2). The data showed identical haplotypes among affected individuals
41 (in contrast to the unaffected individuals) indicating that c.2036A>T probably occurred on the
42 same ancestral allele. Of note, the allele frequency of rs201302247 in Ashkenazi Jews (0.397%)
43 is almost 20 times higher than that in the general population (Genome Aggregation Database;
44 <https://gnomad.broadinstitute.org/variant/6-6152055-T-A>). The incidence of familial multiple
45 dermatofibromas is not known (in any population) but our data indicate that, although rare and
46 perhaps underreported, it may be substantially higher in Ashkenazi Jews.
47
48
49
50
51
52
53
54
55
56
57
58
59
60

Mutations in *F13A1* are not detectable in sporadic dermatofibromas

To explore whether mutations in *F13A1* might also be present in the more common sporadic dermatofibromas, we undertook Sanger sequencing of the coding and promoter regions of *F13A1* using DNA extracted from paraffin-embedded tissue of 22 sporadic single dermatofibromas from unrelated individuals; no potentially deleterious variants were identified (Supplementary Methods and Results, and Tables S3-S6).

The mutation Lys679Met in FXIII-A results in reduced crosslinking activity

To assess the activity of the Lys679Met mutant FXIII-A protein, we generated Glutathione S-Transferase (GST)-fusions of wild-type (WT) or Lys679Met FXIII-A (see Supplementary Table S7 for site directed mutagenesis details), purified recombinant proteins (Figure 2a) and performed pentylamine incorporation into casein assays. We found that the Lys679Met FXIII-A mutation led to reduced crosslinking at 30 min by 50% compared to WT protein (Figure 2b, c). To find possible clues for the altered catalytic activity we looked at the available structural information. Factor XIII-A is composed of five major structural regions: an N-terminal activation peptide (residues 1-38), a β -sandwich domain (residues 39-184), a catalytic domain (185-516), and two β -barrel domains (517-628 and 629-732) that in the inactive FXIII-A zymogen are arranged in a dimer (Figure 2d) (Yee et al., 1994; Weiss et al., 1998). Residue Lys679 is solvent exposed and maps on a β -strand of the second β -barrel domain. In the inactive enzyme, access to active site is occluded by an intramolecular interaction within the first β -barrel domain which, in turn, is stabilized by the N-terminal peptide of the second FXIII-A molecule. Enzyme activation involves thrombin cleavage of the activation peptide in the presence of Ca^{2+} ions, and calcium binding results in dimer destabilization and a large structural

1
2
3 rearrangement involving a swinging movement of both β -barrel domains (Figure 2e). This
4 leads to an active FXIII-A monomer in which the active site is accessible (Stieler et al., 2013).
5
6 In the active conformation observed by crystallography, Lys679 is located away from the active
7 site (more than 63 angstroms (Å)) ruling out a direct effect of the Lys to Met mutation on the
8 catalytic machinery. This mutation could alternatively play a role in the activation mechanism.
9
10 The first five amino acids of the activation peptide are not visible in the structure of the inactive
11 FXIII-A dimer and Lys679 is approximately 22 Å away from the first ordered residue (Arg 6).
12
13 Thus, based on distance considerations, stabilization of the flexible N-terminal peptide by the
14 Lys679Met residue would require some structural rearrangements. We should also point out
15 that in our pentylamine incorporation assay we employed PreScission-cleaved recombinant
16 FXIII-A. Therefore, we cannot exclude that the slightly longer N-terminus resulting from the
17 cloning strategy fortuitously might be stabilized by the Lys679Met mutation more than occurs
18 *in vivo* wherein the Ser2 is expected to be acetylated following cleavage of the first methionine
19 (GPMSETSR.... instead of Ac-SETSR....). More detailed biochemical experiments need to be
20 performed to validate the observed change in catalytic activity and understand its possible
21 molecular basis.
22
23
24
25
26
27
28
29
30
31
32
33
34
35
36
37
38
39
40
41
42
43

44 **The mutation Lys679Met in FXIII-A promotes proliferation and collagen production in** 45 **human dermal fibroblasts**

46
47
48 Proliferation assays were performed to determine whether FXIII-A contributes to fibroblast
49 cell proliferation in dermatofibromas. To expose fibroblasts to FXIII-A, we expressed WT or
50 Lys679Met FXIII-A coupled to GFP by means of an IRES in human embryonic kidney
51 (HEK293) cells and collected secreted protein in the conditioned media. Both WT and
52 Lys679Met constructs yielded similar levels of secreted protein (Figure 3a, inset blot).
53
54
55
56
57
58
59
60

1
2
3 Treatment of fibroblasts with this media demonstrated that incubation with WT FXIII-A led to
4 higher proliferation rates after 48h, whereas Lys679Met FXIII-A led to significantly higher
5 proliferation rates at both 24 and 48h post-incubation (Figure 3a). To determine whether
6 proliferation rates at both 24 and 48h post-incubation (Figure 3a). To determine whether
7 treatment with FXIII-A also altered pro-fibrotic matrix secretion by fibroblasts, collagen I and
8 fibronectin levels were assessed in whole cell lysates. Western blots revealed a significant
9 increase in collagen synthesis in Lys679Met FXIII-A treated cells but not those treated with
10 WT FXIII-A media, compared to controls (Figure 3b), whereas no change in levels of
11 fibronectin were detected between samples (Supplementary Figure S3a). Quantitative PCR
12 analysis further demonstrated upregulation of collagen I mRNA levels in Lys679Met FXIII-A
13 treated cells compared to WT (Figure 3c). To further analyze native ECM deposition by cells,
14 fibroblasts were grown for 14 days on coverslips to generate cell-derived matrix (CDM) in the
15 presence or absence of FXIII-A. Imaging of the resulting CDM preparations revealed an
16 apparent increase in disorganized collagen production in cells treated with Lys679Met FXIII-
17 A compared to WT (Figure 3d). These combined data suggest that FXIII-A can promote
18 fibroproliferative responses in fibroblasts and that the identified Lys679Met mutation enhances
19 this property of FXIII-A.
20
21
22
23
24
25
26
27
28
29
30
31
32
33
34
35
36
37
38
39
40
41
42
43

44 **Lys679Met FXIII-A shows higher association with $\alpha 4\beta 1$ integrins on fibroblasts**

45
46 Our data demonstrated that, in contrast to lower activity as a coagulation factor, Lys679Met
47 FXIII-A exhibited more activity in terms of a fibroproliferation. Previous data have suggested
48 that FXIII-A binds to $\alpha 4\beta 1$ integrin to elicit some cellular activities (Isobe et al., 1999). To
49 explore this possibility, we performed early adhesion assays to collagen I substrates of
50 fibroblasts pre-treated with WT or Lys679Met FXIII-A. Data revealed a significant increase in
51 adhesion of cells treated with Lys679Met FXIII-A compared to WT or control samples (Figure
52
53
54
55
56
57
58
59
60

1
2
3 3e), suggesting enhanced integrin activation in these cells. Given that $\alpha 4\beta 1$ integrin is a
4 fibronectin receptor and does not directly bind to collagen I, other matrix receptors e.g. $\alpha 1\beta 1$,
5 $\alpha 2\beta 1$ integrin may be involved in the binding.
6
7
8
9

10 To investigate whether FXIII-A binds to specific sites on the cell surface, the
11 localization patterns of FXIII-A, $\alpha 4$ and active $\beta 1$ integrins were analyzed in FXIII-A-treated
12 fibroblasts by confocal microscopy. Images and subsequent analysis revealed that active $\beta 1$
13 integrins co-localized with WT FXIII-A and this was significantly increased for Lys679Met
14 FXIII-A (Figure 4a, b). Moreover, levels of active $\beta 1$ integrins were significantly higher in
15 Lys679Met FXIII-A treated cells compared to WT or untreated cells (Figure 4c), further
16 supporting the notion that mutant FXIII-A can activate integrin receptors at the surface of
17 fibroblasts. Similarly, $\alpha 4$ integrins showed a significant increase in co-localization between
18 with Lys679Met FXIII-A compared to WT (Figure 4d, e), indicating that mutant FXIII-A either
19 binds with higher specificity to $\alpha 4$ integrin, or that the protein remains at these sites for longer
20 after binding. No significant difference in levels of total $\alpha 4$ integrin protein were observed
21 between WT and Lys679Met FXIII-A treated cells, (Supplementary Figure S3c, d) suggesting
22 that FXIII-A exerts effects at the level of integrin localization in fibroblasts. This observation
23 suggests FXIII-A associates with integrins and results in increased receptor activation.
24
25
26
27
28
29
30
31
32
33
34
35
36
37
38
39
40
41
42

43 To further investigate whether FXIII-A may co-operate with $\alpha 4\beta 1$ to elicit phenotypic
44 effects, cells were pre-treated with $\alpha 4\beta 1$ -specific inhibitors (BIO1211, BOP and TCS2134)
45 prior to treatment with FXIII-A. Confocal imaging of $\alpha 4\beta 1$ integrins revealed a visible
46 reduction in the levels of both WT and Lys679Met FXIII-A associated with the plasma
47 membrane in cells treated with BIO1211, suggesting active $\alpha 4\beta 1$ is required for FXIII-A
48 binding to the plasma membrane (Figure 5a). Further analysis demonstrated that all three
49 integrin inhibitors suppressed the Lys679Met FXIII-A-dependent increase in collagen
50
51
52
53
54
55
56
57
58
59
60

1
2
3 synthesis (Figure 5b) and proliferation (Figure 5c). These observations suggest that FXIII-A
4
5 requires $\alpha 4$ integrin to associate with the membrane and promote fibroproliferative responses.
6
7

8
9 FXIII-A has previously been suggested to associate with integrins through the
10
11 isoleucine-leucine-aspartate-threonine 'ILDT' amino acid motif located on the catalytic
12
13 domain (Isobe et al., 1999). To test this hypothesis, site-directed mutagenesis was performed
14
15 to mutate the ILDT motif to AAAA in FXIII-A and define the potential role of this site in
16
17 regulating fibro-proliferative phenotypes. We found that mutation of ILDT to AAAA resulted
18
19 in inhibition of the FXIII-A-induced increase in both collagen production and proliferation
20
21 (Figure 5d, e). These data support the notion that FXIII-A can bind to $\alpha 4$ through the ILDT
22
23 motif and that this region may co-operate with the residues around Lys679 to promote $\alpha 4$
24
25 association.
26
27
28
29
30
31
32

33 **FXIII-A regulates mitogen-activated protein kinase (MAPK) and phosphatidylinositol 3** 34 35 **kinase (PI3K) activation**

36
37
38 To further investigate potential mechanisms by which FXIII-A promotes cell proliferation and
39
40 collagen synthesis, we analyzed activation of a range of different signaling pathways in cells
41
42 treated with WT or Lys679Met FXIII-A. Tissue transglutaminase has been reported to promote
43
44 platelet-derived growth factor receptor (PDGFR)-integrin association, and we therefore
45
46 hypothesized that FXIII-A binding may enhance activation of this pathway (Zemskov et al.,
47
48 2009). Western blotting analysis of cells treated with WT or Lys679Met FXIII-A revealed no
49
50 significant increase in PDGFR activity (as judged by pTyr-751 reactivity, Figure 6a). There
51
52 were also no detectable changes in activity of the small guanosine triphosphatase (GTPase)
53
54 RhoA, that is known to be activated downstream of integrins and can contribute to collagen
55
56 synthesis (Supplementary Figure S3e). However, further analysis of other downstream
57
58
59
60

1
2
3 signaling targets (Akt, ERK1/2, p38alpha) revealed that pAkt and pERK both showed
4 significantly increased activation levels in cells following 1h of treatment with both WT and
5 Lys679Met FXIII-A (Figure 6a, b, c). Taken together, these data suggest that FXIII-A can
6 promote activation of Akt and MAPK pathways, which may potentially increase cell
7 proliferation (Figure 6d).
8
9
10
11
12
13
14
15
16
17

18 DISCUSSION

21 Dermatofibroma is a common benign fibro-histiocytic skin tumor but little is known about its
22 pathogenesis (Hsi and Nickoloff, 1996). Typically, dermatofibromas are thought to be induced
23 by trauma, particularly following insect bites. Here, we investigated two unrelated pedigrees
24 with autosomal dominant familial multiple dermatofibromas and identified a heterozygous
25 missense mutation in FXIII-A. On one level this is a surprising finding given that FXIII-A
26 antibodies have been used for the last 40 years for the immunohistochemical diagnosis of
27 dermatofibromas (Cerio et al., 1988). Nevertheless, we also demonstrated that the mutant
28 FXIII-A protein has a functional impact with reduced crosslinking activity but increased
29 fibroblast cell proliferation and adhesion and type I collagen synthesis. Thus, FXIII-A is not
30 only a useful immunohistochemical marker for dermatofibromas but it is also directly
31 implicated in the molecular genetics of families with multiple dermatofibromas, at least in this
32 study.
33
34
35
36
37
38
39
40
41
42
43
44
45
46
47
48

49 FXIII-A is found mainly in macrophages and other cell types including fibroblast-like
50 mesenchymal cells and is expressed in many fibrovascular tumors (Cerio et al., 1989, Nemeth
51 and Penneys, 1989). Indeed, in dermatofibromas, aside from fibroblasts, the main cellular
52 component comprises cells of monocyte/macrophage lineage and it is these cells that mainly
53 express FXIII-A. In addition, FXIII-A is also present in platelet granules (Muszbek et al.,
54
55
56
57
58
59
60

1
2
3 2011). Our working hypothesis, therefore, is that an insect bite or direct trauma may promote
4 a bleed (hemosiderin is common in dermatofibromas, Figure 1c lower image). This bleeding
5 may be enhanced by the presence of Lys679Met FXIII-A which shows reducing clot
6 stabilization function (but no clinical bleeding abnormality). The small bleed then triggers
7 platelet plug formation, platelet granule degradation and release of FXIII-A that then impacts
8 on fibroblast cell biology and collagen production. Still to be explored and currently
9 unexplained, however, is the role of mutant FXIII-A in monocyte/macrophages.
10
11
12
13
14
15
16
17
18
19

20 Previously, autosomal recessive mutations in FXIII-A (mostly A-subunit, rarely B)
21 have been identified in very rare bleeding disorders (incidence ~1 in 5 million), sometimes
22 with wound healing abnormalities (Karimi et al., 2009), but no pathogenic autosomal dominant
23 mutations have been previously described. The mutation Lys679Met is not a novel variant but
24 is present in the general population with low frequency (risk allele frequency 0.0207%;
25 rs201302247); the allele is more common among Ashkenazi Jews (Genome Aggregation
26 Database). Our expectation is that other individuals with this heterozygous missense mutation
27 may also have multiple dermatofibromas, although this remains to be proven. Regarding
28 sporadic, non-familial dermatofibromas, we did not find any evidence for *FI3A1* genetic
29 variants and therefore the role that FXIII-A may play (or not) in such lesions awaits further
30 study.
31
32
33
34
35
36
37
38
39
40
41
42
43
44
45

46 Previous reports have suggested that recessive mutations within the β -barrel 1 and β -
47 barrel 2 domains of FXIII-A can affect the regions of the protein that regulate conformational
48 changes during activation (Thomas et al., 2016). Our analysis suggests that the Lys679Met
49 mutation is more likely to have an impact on the activation step rather than a direct effect on
50 the catalytic machinery. The exact molecular details of how this might occur are not yet clear.
51
52
53
54
55
56
57
58
59
60

1
2
3 Two key phenotypes of dermatofibroma are fibroblast proliferation and collagen
4 production. In contrast to reduced coagulation function, the mutation Lys679Met clearly
5 enhances both pro-fibrotic and proliferative effects, as evidenced by the proliferation data and
6 type I collagen qPCR, western blots and cell-derived matrix production. Our data also suggest
7 that FXIII-A associates with $\alpha4\beta1$ integrins at the plasma membrane to elicit these phenotypic
8 effects and that this is mediated via the ILDT motif in FXIII-A. Lys679Met FXIII-A may bind
9 with a higher affinity or for a greater length of time to $\alpha4$ integrins. However, biochemical *in*
10 *vitro* studies to assess direct binding would be required to validate this hypothesis.
11
12
13
14
15
16
17
18
19
20
21

22 We further explored the link between $\alpha4$ integrin activation and proliferation and
23 collagen synthesis. Published evidence suggests that upon activation, integrins can activate
24 PDGFR or LRP-6 (Muramatsu et al., 2004, Ren et al., 2013, Zemskov et al., 2009) although
25 we did not observe any activation in these receptors. We also did not observe changes to the
26 activity of RhoA upon FXIII-A addition to fibroblasts. We demonstrated significant increases
27 in pERK1/2 and pAkt upon FXIII-A binding, which are key downstream targets in the
28 RAS/RAF/MEK/ERK and the PI3K/Akt signaling pathways, but there were no differences
29 between WT and Lys679Met (De Luca et al., 2012). For now, we conclude that the proposed
30 enhanced action of Lys679Met FXIII-A on $\alpha4$ integrin could initiate different signaling
31 cascades which remain to be determined (Figure 6d).
32
33
34
35
36
37
38
39
40
41
42
43
44
45

46 In summary, our study provides insight into the genetic and cellular basis of a subset of
47 familial dermatofibromas and highlight an extended role for FXIII-A in their pathobiology.
48
49
50

51 MATERIALS AND METHODS

52
53
54
55
56
57
58
59

60 Whole Exome Sequencing (WES) and Sanger Sequencing

1
2
3 Following informed consent from the patients and ethics committee approval, WES was
4 performed using DNA from available probands and their family members by the Illumina
5 HiSeq2500 system (Illumina, San Diego, CA). The Exome capture kit (Agilent SureSelect
6 Human All Exon 50 Mb kit, Santa Clara, CA) was used to prepare DNA libraries from 3 µg of
7 DNA. First, the Adapted Focused Acoustic technology (Covaris, Woburn, MA) was used to
8 shear genomic DNA to yield a mean of 150bp fragment size. The fragment ends were then
9 repaired, ligated with sequencing adaptors and hybridized against biotinylated 120bp RNA
10 probes (Agilent) targeting protein-coding genomic regions for 24 hours. Targeted regions were
11 selected for with magnetic streptavidin-coated beads while unbound DNA was washed off. The
12 exome-enriched DNA pool was next eluted, amplified with low-cycle PCR, multiplexed (4
13 samples on each lane) and sequenced with 100bp paired-end reads. Reads were aligned to the
14 GRCh37/hg19 reference genome using Novoalign (Novocraft Technologies, Selangor,
15 Malaysia). The Bedtools package and custom scripts were used to calculate the depth of
16 sequence coverage (Quinlan and Hall, 2010). The SAMtools software was used for variant
17 calling and quality filtering (Li et al., 2009). Variants were then annotated with multiple passes
18 through the ANNOVAR software package (Wang et al., 2010). PCR and Sanger sequencing
19 were performed to validate the segregation of the mutation with phenotypes according to
20 standard protocol using primers for *F13A1* exon14 (Supplementary Tables S5).

21 22 23 24 25 26 27 28 29 30 31 32 33 34 35 36 37 38 39 40 41 42 43 44 45 46 47 48 **Purification of FXIII-A- GST fusion proteins for functional analysis**

49
50
51 pGEX-FXIII-A, an expression vector encoding an N-terminal GST-FXIII-A fusion protein,
52 was generated as previously described (Smith et al., 2011). Lys679Met FXIII-A variant was
53 generated by site-directed mutagenesis using the listed primers (Supplementary Table S7) with
54 QuickChange II Kit (Agilent Technologies; Stockport, UK). Successful mutagenesis was
55
56
57
58
59
60

1
2
3 verified by DNA sequencing. Both FXIII-A plasmids were then transformed into XL10-Gold®
4 Ultra-competent *E. Coli* (Agilent Technologies, Wokingham, UK). FXIII-A₂ Expression and
5
6 purification were performed as previously described (Duval et al., 2016).
7
8
9
10
11
12

13 **FXIII-A activity analysis by Pentylamine Incorporation**

14
15
16 Measurement of FXIII activity was performed using a modified 5-(biotinamido) pentylamine
17 incorporation assay. Nunc-Immuno- 96 Micro-Well plates were coated with 100µl of 10µg/ml
18 N, N-dimethylated casein overnight at 4°C, then blocked with 300µl 1% BSA in Tris buffer
19 saline (TBS) for 90min at 37°C. Plates were then washed with 4x 300µl TBS and 10µl of
20 samples (WT or Lys679Met rhFXIII-A₂ or murine plasma) were added to the wells in triplicate.
21
22 90µl of activation mix (111µM dithiothreitol, 0.3µM biotinylated pentylamine, 11mM CaCl₂,
23 2.2U/ml thrombin) was added and the reactions were stopped at 0, 20, 40, 60, 80, 100, 120 min
24 by adding 200µl of 200mM EDTA. Plates were washed with 4x 300µl 0.1% [v/v] Tween20 in
25 TBS, and 100µl of 2µg/ml of streptavidin in 1% [w/v] BSA (in TBS-Tween) were added for
26 60min at 37°C. Following washes with 4x 300µl TBS-Tween, 100µl of 1mg/ml phosphatase
27 substrate (in 1M diethanolamine) were added, and the reaction was stopped by adding 100µl
28 of 4M NaOH. Absorbency was measured at 405nm, using a SpectraMax 190 absorbance
29 microtiter plate reader (Molecular Devices, Wokingham, UK). The rate of pentylamine
30 incorporation over time was then used as an indicator of PreScission-cleaved FXIII activity.
31
32 Experiments were performed in triplicate.
33
34
35
36
37
38
39
40
41
42
43
44
45
46
47
48
49
50
51
52
53
54

55 **Normal human dermal fibroblast (NHDF) and HEK293 cell culture**

56
57 NHDFs (Cellworks, Buckingham, UK) up to passage number 10 and HEK293 cell (ATCC;
58 Middlesex, UK) were cultured in DMEM in high glucose (4.5g/L), 10 % (v/v) fetal bovine
59
60

1
2
3 serum (FBS), 50µg/ml penicillin and 2mM L-glutamine in a humidified incubator at 37°C with
4
5 5%CO₂. Cells were tested for Mycoplasma infection with Mycoalert™ Mycoplasma Detection
6
7 Kit (Lonza, Slough, UK).
8
9

10 11 12 13 **Plasmids constructs, site directed mutagenesis and FXIII-A expression in HEK293 cell** 14 15 **line**

16
17
18
19 Site-directed mutagenesis was performed on the mammalian expression vector pIRES2-EGFP
20
21 expression vector containing the cDNA FXIII-A (a kind gift from Consuelo González-
22
23 Manchón, Madrid; Jayo et al., 2009) according to the QuikChange Lightning Site-Directed
24
25 Mutagenesis Kit protocol (Agilent Technologies) using primers (Supplementary Table S7).
26
27 Transient transfection was performed using Lipofectamine 3000 on HEK293 Cell line.
28
29 Transfected cells were grown in 2% FBS containing media for 48 hours before collecting the
30
31 conditioned media for experiments. FXIII-A expression level was verified by Western blotting.
32
33
34
35
36
37
38

39 **Proliferation, adhesion assays and cell-derived matrix (CDM) preparation**

40
41 Fibroblasts were plated in media containing 2% serum a day before the experiment. Cells then
42
43 were treated with conditioned media containing either WT or Lys679Met FXIII-A for 24 and
44
45 48 hours for proliferation assay. Collagen type I solution from rat tail (Sigma-Aldrich) at a
46
47 concentration of 50µg/ml was used to coat a plate for adhesion assays. For CDM preparation,
48
49 cells were grown on 0.2% crosslinked gelatin-coated coverslips for 14 days before cell
50
51 denudation, as previously described (Kaukonen et al., 2017). Cells and matrices were then fixed
52
53 for 10 minutes at room temperature with 4% final concentration of paraformaldehyde. Cells
54
55 were permeabilized with 0.1% Triton-X100 in phosphate buffered saline (PBS) solution for 10
56
57 minutes followed by 1-hour incubation with 3% BSA in PBS solution containing 1:400
58
59
60

1
2
3 phalloidin-AlexaFluor488 and 1:1000 DAPI. The images of cells were acquired by tile-scans
4
5 of each well using EVOSTM FL Auto 2 Imaging System (ThermoFisher, Waltham, MA) with
6
7 a 10x objective lens. The number of cells in each well was measured by automated nuclei
8
9 counting using ImageJ.
10
11
12
13
14
15

16 **Reverse Transcription PCR**

17
18
19 Fibroblasts were treated with WT and Lys679Met FXIII-A for 48 hours. Total RNA was
20
21 extracted using RNeasy Micro Kit (Qiagen). The quality of RNA was analyzed by the
22
23 Nanodrop spectrophotometer (ThermoFisher). Reverse Transcription was performed using
24
25 High-Capacity cDNA Reverse Transcription Kit according to the manufacturer's protocol.
26
27 Gene expression was assessed by real-time PCR by using TagMan® Gene Expression Assays
28
29 for *Coll1a1* Mm00801666_g1 (ThermoFisher). Transcript levels were normalized to GAPDH
30
31 expression, measured with Applied Biosystems (Foster City, CA) TaqMan probes.
32
33
34
35
36
37
38
39

40 **Western blot analysis**

41
42 Whole-cell lysates of fibroblasts were collected after treatment with FXIII-A conditioned
43
44 media using RIPA buffer with protease inhibitor cocktail set I (Calbiochem, San Diego, CA).
45
46 Each sample was resuspended in NuPAGE™ LDS Sample Buffer (Invitrogen™), boiled at
47
48 100°C for 5 minutes and run on NuPAGE™ 4-12% Bis-Tris Protein Gels (Invitrogen™).
49
50 Resolved proteins were transferred and blotted onto nitrocellulose membrane. Primary and
51
52 secondary antibodies are listed (Supplementary Table S8).
53
54
55
56
57
58
59

60 **Immunofluorescence and confocal microscopy**

1
2
3 Fibroblasts on coverslips were treated with WT and Lys679Met FXIII-A over variable time
4
5 points, then washed and fixed with 4% paraformaldehyde in PBS before 10-minute
6
7 permeabilization with 0.1% Triton-X100, followed by blocking with 5% BSA in PBS for 30
8
9 minutes. Cells were labelled with antibodies (Supplementary Table S8) at 4°C overnight and
10
11 then stained with secondary antibodies (Supplementary Table S8), phalloidin-AlexaFluor568
12
13 and DAPI. Cells were imaged with 60x objective using Nikon A1R inverted confocal
14
15 microscope. Images were exported from Nikon Elements software for further analysis in
16
17 ImageJ software using intensity functions of the co-localization analysis plugin JaCoP.
18
19
20
21
22
23
24

25 **Data Availability Statement**

26
27
28 Datasets related to this article can be found at [https://www.ncbi.nlm.nih.gov/bioproject/](https://www.ncbi.nlm.nih.gov/bioproject/PRJNA545215)
29
30 PRJNA545215, hosted at Sequence Read Archive (SRA) under the collection ID
31
32 PRJNA545215.
33
34
35
36
37
38
39

40 **Conflict of Interest**

41
42 The authors have no conflicts of interest to declare.
43
44
45
46
47

48 **Acknowledgements**

49
50 The authors acknowledge financial support from Rosetrees Trust, Medical Research Council
51
52 UK (MR/M018512/1) and the National Institute for Health Research (NIHR) Biomedical
53
54 Research Centre based at Guy's and St Thomas' NHS Foundation Trust, King's College
55
56 London, U.K and Department of Medical Services, Ministry of Public Health, Thailand.
57
58
59
60

CRedit statement

Conceptualization, C.S., M.P. and J.A.M. Investigation, C.S., C.K.H., M.M., C.D., J.Y.W.L., T.C., R.S., R.A.S.A and M.P. Formal Analysis, C.S. C.K.H, C.D., T.C., A.O., M.A.S., J.E.C and M.P. Methodology, C.S., C.K.H., M.P. Resources, H-S.Y., H-Y. H., O.S., E.S., M.S-E, Cu.S. Supervision, M.P., J.A.M. Writing, original draft, C.S. Writing, review & editing, C.S., M.P. and J.A.M.

REFERENCES

- Altman DA, Nickoloff BJ, Fivenson DP. Differential expression of factor XIIIa and CD34 in cutaneous mesenchymal tumors. *J Cutan Pathol* 1993;20:154-8.
- Bagoly Z, Katona E, Muszbek L. Factor XIII and inflammatory cells. *Thromb Res* 2012;129 Suppl 2:S77-81.
- Beatrous SV, Riahi RR, Grisoli SB, Cohen PR. Associated conditions in patients with multiple dermatofibromas: Case reports and literature review. *Dermatol Online J* 2017;23.
- Cerio R, Griffiths CE, Cooper KD, Nickoloff BJ, Headington JT. Characterization of factor XIIIa positive dermal dendritic cells in normal and inflamed skin. *Br J Dermatol* 1989;121:421-31.
- Cerio R, Spaul J, Jones EW. Identification of factor XIIIa in cutaneous tissue. *Histopathology* 1988;13:362-4.
- De Luca A, Maiello MR, D'Alessio A, Pergameno M, Normanno N. The RAS/RAF/MEK/ERK and the PI3K/AKT signalling pathways: role in cancer pathogenesis and implications for therapeutic approaches. *Expert Opin Ther Targets* 2012;16 Suppl 2:S17-27.

- 1
2
3 Duval C, Ali M, Chaudhry WW, Ridger VC, Ariens RA, Philippou H. Factor XIII A-Subunit
4 V34L Variant Affects Thrombus Cross-Linking in a Murine Model of Thrombosis.
5 Arterioscler Thromb Vasc Biol 2016;36:308-16.
6
7
8
9
10 Hsi ED, Nickoloff BJ. Dermatofibroma and dermatofibrosarcoma protuberans: an
11 immunohistochemical study reveals distinctive antigenic profiles. J Dermatol Sci
12 1996;11:1-9.
13
14
15
16
17 Isobe T, Takahashi H, Ueki S, Takagi J, Saito Y. Activity-independent cell adhesion to tissue-
18 type transglutaminase is mediated by alpha4beta1 integrin. Eur J Cell Biol
19 1999;78:876-83.
20
21
22
23
24 Jakobiec FA, Rai R, Yoon MK. Fibrous histiocytoma of the tarsus: clinical and
25 immunohistochemical observations with a differential diagnosis. Cornea 2014;33:536-
26 9.
27
28
29
30 Jakobiec FA, Zakka FR, Tu Y, Freitag SK. Dermatofibroma of the Eyelid:
31 Immunohistochemical Diagnosis. Ophthal Plast Reconstr Surg 2017;33:e134-8.
32
33
34
35 Jayo A, Conde I, Lastres P, Jimenez-Yuste V, Gonzalez-Manchon C. Possible role for cellular
36 FXIII in monocyte-derived dendritic cell motility. Eur J Cell Biol 2009;88:423-31.
37
38
39
40 Kaukonen R, Jacquemet G, Hamidi H, Ivaska J. Cell-derived matrices for studying cell
41 proliferation and directional migration in a complex 3D microenvironment. Nat Protoc
42 2017;12:2376-90.
43
44
45
46
47
48 Karimi M, Bereczky Z, Cohan N, Muszbek L. Factor XIII Deficiency. Semin Thromb Hemost
49 2009;35:426-38.
50
51
52 Kluger N, Cotten H, Magana C, Piquier L. Dermatofibroma occurring within a tattoo: report
53 of two cases. J Cutan Pathol 2008;35:696-8.
54
55
56
57 Komaromi I, Bagoly Z, Muszbek L. Factor XIII: novel structural and functional aspects. J
58 Thromb Haemost 2011;9:9-20.
59
60

- 1
2
3 Li H, Handsaker B, Wysoker A, Fennell T, Ruan J, Homer N, et al. The Sequence
4 Alignment/Map format and SAMtools. *Bioinformatics* 2009;25:2078-9.
5
6
7
8 Muramatsu H, Zou P, Suzuki H, Oda Y, Chen GY, Sakaguchi N, et al. alpha4beta1- and
9
10 alpha6beta1-integrins are functional receptors for midkine, a heparin-binding growth
11
12 factor. *J Cell Sci* 2004;117:5405-15.
13
14
15 Muszbek L, Berezky Z, Bagoly Z, Komaromi I, Katona E. Factor XIII: a coagulation factor
16
17 with multiple plasmatic and cellular functions. *Physiol Rev* 2011;91:931-72.
18
19
20 Myers DJ, Fillman EP. Dermatofibroma. [Updated 2019 Feb 15]. In: StatPearls [Internet].
21
22 Treasure Island (FL): StatPearls Publishing; 2019; Available from:
23
24 <https://www.ncbi.nlm.nih.gov/books/NBK470538/>
25
26
27 Nemeth AJ, Penneys NS. Factor XIIIa is expressed by fibroblasts in fibrovascular tumors. *J*
28
29 *Cutan Pathol* 1989;16:266-71.
30
31
32 Quinlan AR, Hall IM. BEDTools: a flexible suite of utilities for comparing genomic features.
33
34 *Bioinformatics* 2010;26:841-2.
35
36
37 Ren S, Johnson BG, Kida Y, Ip C, Davidson KC, Lin SL, et al. LRP-6 is a coreceptor for
38
39 multiple fibrogenic signaling pathways in pericytes and myofibroblasts that are
40
41 inhibited by DKK-1. *Proc Natl Acad Sci U S A* 2013;110:1440-5.
42
43
44 Samlaska C, Bennion S. Eruptive dermatofibromas in a kindred. *Cutis* 2002; 69:187-8,190.
45
46
47 Smith KA, Adamson PJ, Pease RJ, Brown JM, Balmforth AJ, Cordell PA, et al. Interactions
48
49 between factor XIII and the alpha C region of fibrinogen. *Blood* 2011;117:3460-8.
50
51
52 Stieler M, Weber J, Hils M, Kolb P, Heine A, Büchold C, et al. Structure of active coagulation
53
54 factor XIII triggered by calcium binding: basis for the design of next-generation
55
56 anticoagulants. *Angew Chem Int Ed Engl* 2013;52:11930-4.
57
58
59
60

- 1
2
3 Thomas A, Biswas A, Dodt J, Philippou H, Hethershaw E, Ensikat HJ, et al. Coagulation factor
4
5 XIII A subunit missense mutations affect structure and function at the various steps of factor
6
7 XIII action. *Hum Mutat* 2016;37:1030-41.
8
9
10 Wang K, Li M, Hakonarson H. ANNOVAR: functional annotation of genetic variants from
11
12 high-throughput sequencing data. *Nucleic Acids Res* 2010;38:e164.
13
14 Weiss MS, Metzner HJ, Hilgenfeld R. Two non-proline cis peptide bonds may be important
15
16 for factor XIII function. *FEBS Lett.* 1998;423:291-6.
17
18
19 Yee VC, Pedersen LC, Le Trong I, Bishop PD, Stenkamp RE, Teller DC. Three-dimensional
20
21 structure of a transglutaminase: human blood coagulation factor XIII. *Proc Natl Acad*
22
23 *Sci U S A.* 1994;91:7296-300.
24
25
26
27 Zelger BG, Zelger B. Dermatofibroma. A clinico-pathologic classification scheme. *Pathologie*
28
29 1998;19:412-9.
30
31
32 Zemskov EA, Loukinova E, Mikhailenko I, Coleman RA, Strickland DK, Belkin AM.
33
34 Regulation of platelet-derived growth factor receptor function by integrin-associated
35
36 cell surface transglutaminase. *J Biol Chem* 2009;284:16693-703.
37
38
39
40
41
42

43 **Figure legends:**

45 **Figure 1: Clinicopathologic and molecular basis of familial multiple dermatofibromas.**

47 (a) Pedigrees of the two families showing all affected individuals with the *F13A1* mutation
48 c.2036A>T (Lys679Met). (b) Multiple dermatofibromas in Family 1 individual II-2 (left) and
49 Family 2 individuals II-3 (right). (c) Histopathologic features of an excised dermatofibromas
50 from an individual II-2 in Family 1 showing proliferation of fibro-histiocytic cells within the
51 dermis with an overlying Grenz zone (left image; hematoxylin and eosin, $\times 4$; scale bar 500 μ m
52
53
54
55
56
57
58
59
60

1
2
3). There is collagen entrapment at the periphery of the lesion as well as presence of hemosiderin
4
5 pigment (right image; hematoxylin and eosin, $\times 10$; scale bar 200 μ m).
6
7
8
9

10
11 **Figure 2: Mutation Lys679Met in FXIII-A leads to reduced protein activity** (a) SDS PAGE
12 gel showing purity and levels of WT and Lys679Met FXIII-A purified recombinant proteins
13 used in the assay. (b) Graph showing rate of pentylamine incorporation over time in
14 preparations containing WT or Lys679Met mutant protein. (c) Percentage biotin incorporation
15 as an estimation of FXIII activity. The data display means \pm SD for three experiments. *** =
16 $p=0.0007$. (d) Cartoon representation of the inactive FXIII-A dimer (PDB code 1F13). For one
17 FXIII-A molecule distinct structural regions are labeled and highlighted using different colors.
18 The second FXIII-A molecule is shown in grey. Residue Lys679 is shown as stick
19 representation in black. Residues of the catalytic triad are shown in orange. Lys679 is located
20 ~ 22 Å away from the first ordered residue of the N-terminal activation peptide. (e) Cartoon
21 representation of Ca²⁺-activated FXIII-A monomer (PDB code 4KTY) shown in the same
22 orientation as in (d) Color-codes for the distinct structural regions are the same as in (d). The
23 inhibitor bound in the active site is shown in cyan. Calcium ions are shown as grey spheres.
24 Residue Lys679 is shown as stick representation in black. Ca²⁺-induced activation elicits a
25 large swinging movement of the β -barrel domains. In this conformation Lys679 is located ~ 63
26 Å away from the active site.
27
28
29
30
31
32
33
34
35
36
37
38
39
40
41
42
43
44
45
46
47
48
49
50
51

52 **Figure 3: Mutation Lys679Met in FXIII-A leads to increased fibroblast proliferation,**
53 **collagen production and changes in extracellular matrix organization.** (a) Graph shows
54 that NHDF proliferation is increased for Lys679Met FXIII-A compared to WT FXIII-A at both
55 24 and 48 hours. (b) Collagen I western blot and (c) qPCR show that Lys679Met FXIII-A
56
57
58
59
60

1
2
3 promotes more collagen I production after 48 hours compared to WT FXIII-A. **(d)** Images of
4 CDM produced by cells showing those treated with Lys679Met FXIII-A express more collagen
5 made of thickened fibers compared to WT FXIII-A (scale bars 10um). **(e)** Adhesion assay
6
7 showing number of cells adhering to collagen I-coated plate at 1 hour is greater for Lys679Met
8 FXIII-A compared to WT FXIII-A. The data indicate means +/- SD for three experiments* =
9
10
11
12
13
14
15
16
17
18
19
20
21
22
23
24
25
26
27
28
29
30
31
32
33
34
35
36
37
38
39
40
41
42
43
44
45
46
47
48
49
50
51
52
53
54
55
56
57
58
59
60

p<0.05 * * = p<0.01 vs control, *** = p<0.001 vs control. All experiments were done in triplicate (n=3). C, W and M indicates control, wild type or mutant, respectively.

Figure 4: Co-localization of $\alpha 4$, $\beta 1$ and FXIII-A on the cell surface suggests FXIII-A binds to $\alpha 4\beta 1$ integrin Immunofluorescence staining and confocal microscopy of fixed, permeabilized NHDFs on coverslips after treatment with WT FXIII-A or Lys679Met FXIII-A for 2 hours before fixation. **(a)** Images show co-localization of active $\beta 1$ integrin and FXIII-A after treatment with either WT or mutant FXIII-A (scale bars 10um). **(b)** Manders overlap co-efficient analysis showing percentage overlap between FXIII-A and active $\beta 1$ integrin is greater for Lys679Met FXIII-A. **(c)** Level of Active $\beta 1$ integrin intensity per cell is greater for Lys679Met FXIII-A. **(d)** Images show co-localization of $\alpha 4$ integrin and FXIII-A which is greater for Lys679Met FXIII-A compared to WT FXIII-A (scale bars 10um). **(e)** Manders overlap co-efficient analysis showing percentage overlap between FXIII-A and integrin is greater for Lys679Met FXIII-A. All experiments were done in triplicate. The data represent means +/- SD for three experiments* = p<0.05 vs control ** = p<0.01 vs control *** = p<0.001 vs control

Figure 5: FXIII-A associates with $\alpha 4\beta 1$ integrin via the ILDT motif in FXIII-A. **(a)** NHDFs on coverslips were pre-treated with either DMSO (control) or BIO1211 ($\alpha 4\beta 1$ integrin inhibitor) for 2 hours and then WT FXIII-A, Lys679Met FXIII-A and control conditioned

1
2
3 media was added for 1 hour. Confocal images show that BIO1211 induces internalization of
4 $\alpha 4$ integrin (small green dots); there is less FXIII-A binding for both WT and Lys679Met
5 FXIII-A when cells are incubated with BIO1211 (scale bars 10um). (b) Western blots show
6 reduction in collagen I expression after incubation with 3 different integrin inhibitors (BIO1211,
7 BOP, TCS2314), particularly for cells treated with Lys679Met FXIII-A compared to WT
8 FXIII-A. (c) Graph shows reduced cell proliferation rates following FXIII-A treatment (WT or
9 Lys679Met) compared to control after incubation with the 3 integrin inhibitors at 48 hours. (d)
10 Western blot shows reduction of Collagen I expression after 48-hour treatment with
11 ILDT235_238AAAA FXIII-A. (e) Graph shows reduced cell proliferation rate after site-
12 directed mutagenesis of ILDT motif of FXIII-A. These effects for (f) and (g) are common to
13 the WT and Lys679Met FXIII-A but are more marked with Lys679Met FXIII-A. Experiments
14 were performed in triplicate. The data show means +/- SD for three experiments* = $p < 0.05$ vs
15 control ** = $p < 0.01$ vs control *** = $p < 0.001$ vs control. C, W and M indicates control, wild
16 type or mutant, respectively.

17
18
19
20
21
22
23
24
25
26
27
28
29
30
31
32
33
34
35
36
37
38
39 **Figure 6: WT and Lys679Met FXIII-A both increase Akt and ERK1/2 activation.** (a)
40 NHDFs were treated with FXIII-A for 1, 4, or 8 hours with 2 nM PDGF-BB treatment as a
41 positive control. Activation levels of PDGFR and Akt were determined by immunoblotting
42 with antibodies to Tyr (p)-751-PDGFR β and Ser(p)-473-Akt1. All samples were normalized
43 for equal amount with glyceraldehyde-3-phosphate dehydrogenase (GAPDH). No activation
44 was noted for p-PDGFR whereas both WT and Lys679Met FXIII-A showed transient increase
45 in p-Akt signaling at 1 hour. (b) Activation level of LRP-6, ERK1/2 and p38 α were determined
46 by immunoblotting with antibodies to Ser (p)-1490-LRP6, Thr202 (p)/Thr204 (p)-
47 p44/42MAPK (ERK1/2) and Thr (p)-180)/Tyr (p)-182-p38 α . All samples were normalized for
48 equal amounts with GAPDH. Both WT and Lys679Met FXIII-A showed transient increase in
49
50
51
52
53
54
55
56
57
58
59
60

1
2
3 p-ERK1/2 signaling at 1 hour. (c) Phosphoproteins were quantified, averaged and expressed
4 for NHDF cells treated with WT and Lys679Met FXIII-A as fold change over those of
5 untreated cells. Both WT and Lys679Met FXIII-A showed similar ~two-fold increases in p-
6 Akt and p-ERK1/2 compared to control. Shown are the means +/- SD for three experiments.
7
8 (d) A proposed schematic figure for FXIII-A and $\alpha 4\beta 1$ integrins association on the cell surface
9 and downstream signaling. Lys679Met may lead to a conformational change in the protein
10 which promotes $\alpha 4$ integrin binding (right panel). WT and Lys679Met FXIII-A after
11 association with integrins activate Akt and Erk1/2 resulting in cell proliferation, adhesion and
12 collagen production. However, the enhanced action of mutant FXIII-A on $\alpha 4$ integrin could
13 initiate different signaling cascades which still remain to be determined.
14
15
16
17
18
19
20
21
22
23
24
25
26
27
28
29
30
31
32
33
34
35
36
37
38
39
40
41
42
43
44
45
46
47
48
49
50
51
52
53
54
55
56
57
58
59
60

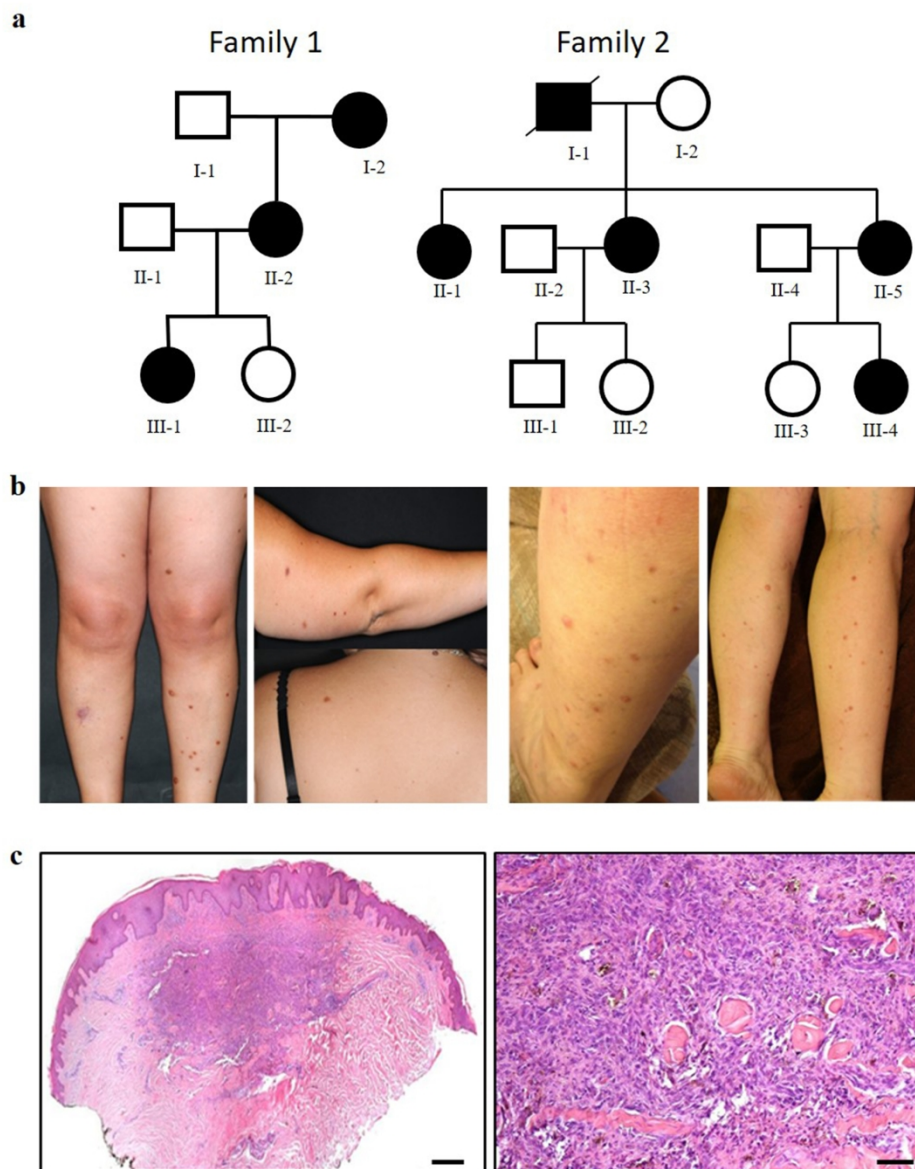


Figure 1: Clinicopathologic and molecular basis of familial multiple dermatofibromas. (a) Pedigrees of the two families showing all affected individuals with the F13A1 mutation c.2036A>T (Lys679Met). (b) Multiple dermatofibromas in Family 1 individual II-2 (left) and Family 2 individuals II-3 (right). (c) Histopathologic features of an excised dermatofibromas from an individual II-2 in Family 1 showing proliferation of fibrohistiocytic cells within the dermis with an overlying Grenz zone (left image; hematoxylin and eosin, $\times 4$; scale bar $500\mu\text{m}$). There is collagen entrapment at the periphery of the lesion as well as presence of hemosiderin pigment (right image; hematoxylin and eosin, $\times 10$; scale bar $200\mu\text{m}$).

179x221mm (300 x 300 DPI)

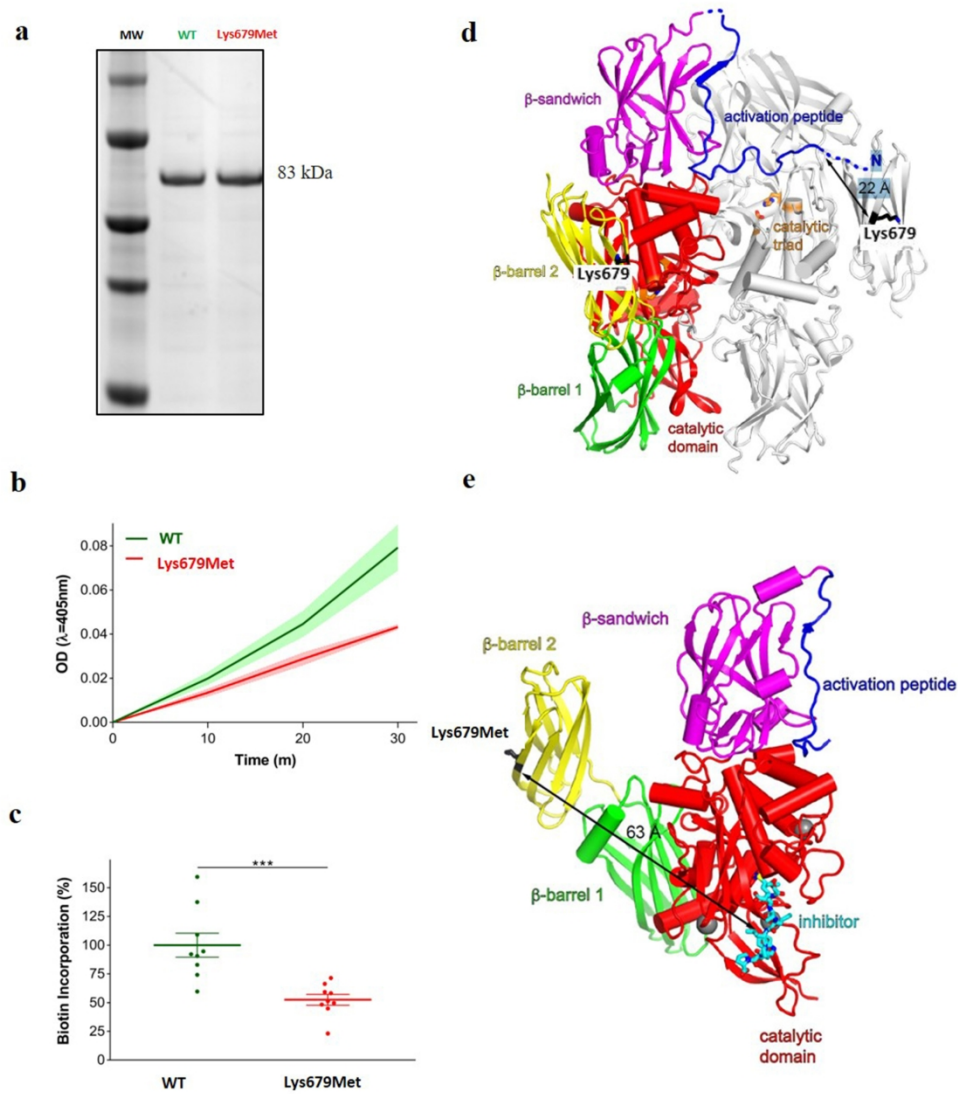


Figure 2: Mutation Lys679Met in FXIII-A leads to reduced protein activity (a) SDS PAGE gel showing purity and levels of WT and Lys679Met FXIII-A purified recombinant proteins used in the assay. (b) Graph showing rate of pentylamine incorporation over time in preparations containing WT or Lys679Met mutant protein. (c) Percentage biotin incorporation as an estimation of FXIII activity. The data display means \pm SD for three experiments. *** = $p=0.0007$. (d) Cartoon representation of the inactive FXIII-A dimer (PDB code 1F13). For one FXIII-A molecule distinct structural regions are labeled and highlighted using different colors. The second FXIII-A molecule is shown in grey. Residue Lys679 is shown as stick representation in black. Residues of the catalytic triad are shown in orange. Lys679 is located ~ 22 Å away from the first ordered residue of the N-terminal activation peptide. (e) Cartoon representation of Ca^{2+} -activated FXIII-A monomer (PDB code 4KTY) shown in the same orientation as in (d) Color-codes for the distinct structural regions are the same as in (d). The inhibitor bound in the active site is shown in cyan. Calcium ions are shown as grey spheres. Residue Lys679 is shown as stick representation in black. Ca^{2+} -induced activation elicits a large swinging movement of the β -barrel domains. In this conformation Lys679 is located ~ 63 Å away from the active site.

1
2
3
4
5
6
7
8
9
10
11
12
13
14
15
16
17
18
19
20
21
22
23
24
25
26
27
28
29
30
31
32
33
34
35
36
37
38
39
40
41
42
43
44
45
46
47
48
49
50
51
52
53
54
55
56
57
58
59
60

184x212mm (300 x 300 DPI)

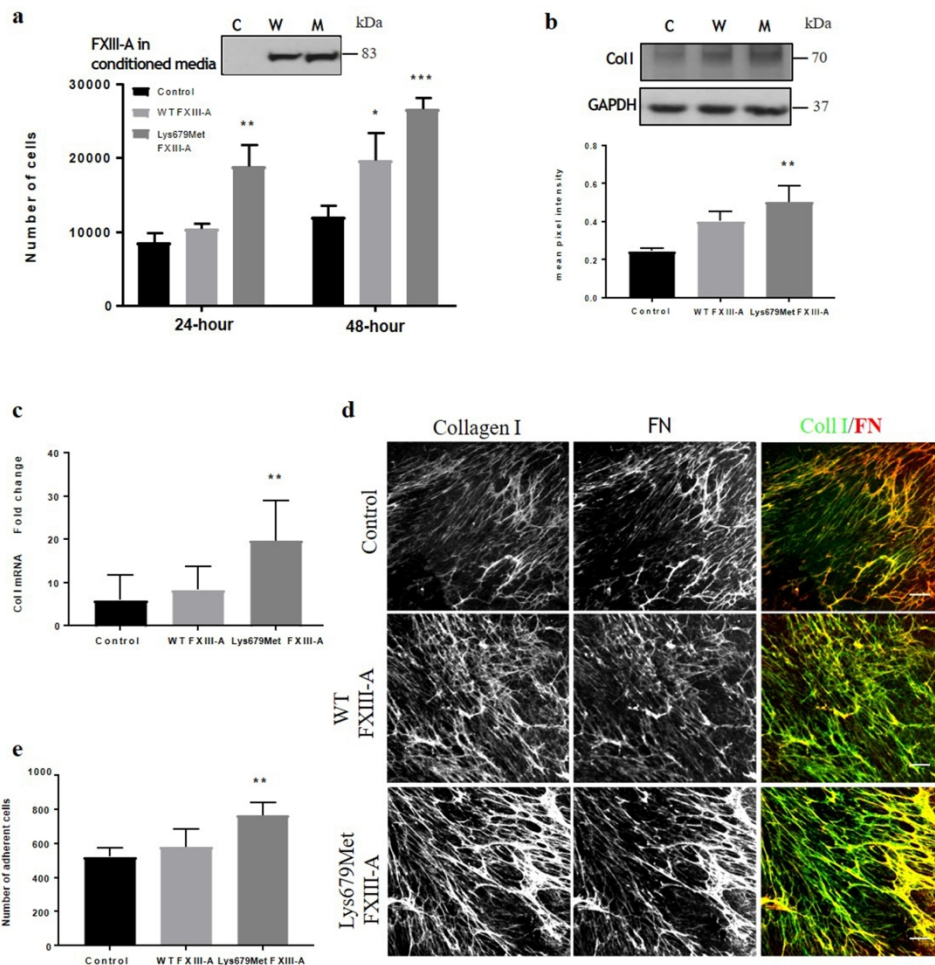


Figure 3: Mutation Lys679Met in FXIII-A leads to increased fibroblast proliferation, collagen production and changes in extracellular matrix organization. (a) Graph shows that NHDF proliferation is increased for Lys679Met FXIII-A compared to WT FXIII-A at both 24 and 48 hours. (b) Collagen I western blot and (c) qPCR show that Lys679Met FXIII-A promotes more collagen I production after 48 hours compared to WT FXIII-A. (d) Images of CDM produced by cells showing those treated with Lys679Met FXIII-A express more collagen made of thickened fibers compared to WT FXIII-A (scale bars 10um). (e) Adhesion assay showing number of cells adhering to collagen I-coated plate at 1 hour is greater for Lys679Met FXIII-A compared to WT FXIII-A. The data indicate means \pm SD for three experiments * = $p < 0.05$ ** = $p < 0.01$ vs control, *** = $p < 0.001$ vs control. All experiments were done in triplicate ($n = 3$). C, W and M indicates control, wild type or mutant, respectively.

198x208mm (300 x 300 DPI)

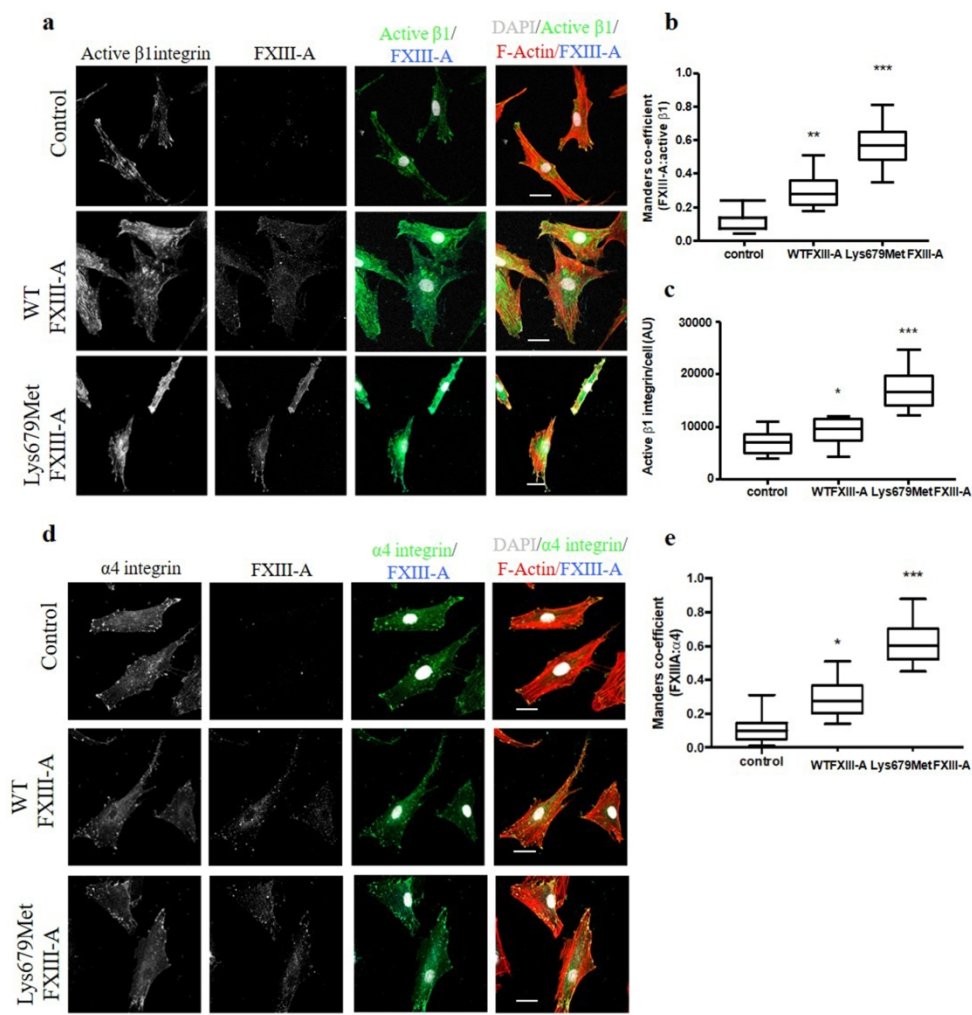


Figure 4: Co-localization of α 4, β 1 and FXIII-A on the cell surface suggests FXIII-A binds to α 4 β 1 integrin. Immunofluorescence staining and confocal microscopy of fixed, permeabilized NHDFs on coverslips after treatment with WT FXIII-A or Lys679Met FXIII-A for 2 hours before fixation. (a) Images show co-localization of active β 1 integrin and FXIII-A after treatment with either WT or mutant FXIII-A (scale bars 10 μ m). (b) Manders overlap co-efficient analysis showing percentage overlap between FXIII-A and active β 1 integrin is greater for Lys679Met FXIII-A. (c) Level of Active β 1 integrin intensity per cell is greater for Lys679Met FXIII-A. (d) Images show co-localization of α 4 integrin and FXIII-A which is greater for Lys679Met FXIII-A compared to WT FXIII-A (scale bars 10 μ m). (e) Manders overlap co-efficient analysis showing percentage overlap between FXIII-A and integrin is greater for Lys679Met FXIII-A. All experiments were done in triplicate. The data represent means +/- SD for three experiments * = $p < 0.05$ vs control ** = $p < 0.01$ vs control *** = $p < 0.001$ vs control

188x196mm (300 x 300 DPI)

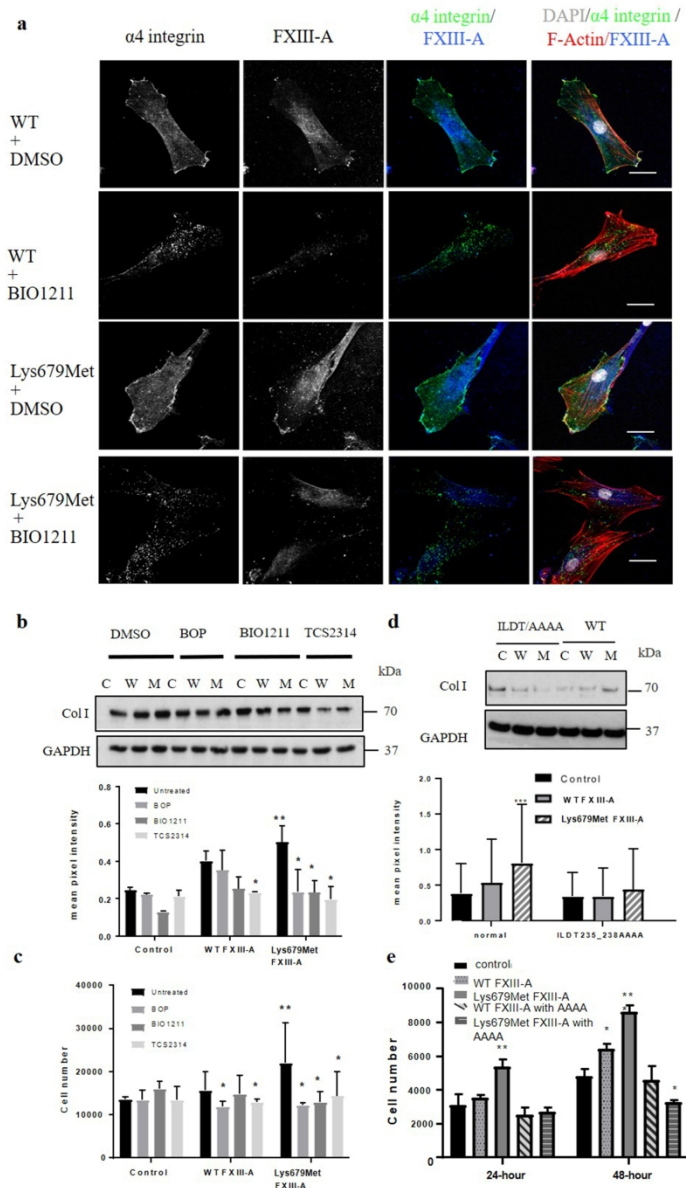


Figure 5: FXIII-A associates with $\alpha 4 \beta 1$ integrin via the ILDT motif in FXIII-A. (a) NHDFs on coverslips were pre-treated with either DMSO (control) or BIO1211 ($\alpha 4 \beta 1$ integrin inhibitor) for 2 hours and then WT FXIII-A, Lys679Met FXIII-A and control conditioned media was added for 1 hour. Confocal images show that BIO1211 induces internalization of $\alpha 4$ integrin (small green dots); there is less FXIII-A binding for both WT and Lys679Met FXIII-A when cells are incubated with BIO1211 (scale bars 10 μ m). (b) Western blots show reduction in collagen I expression after incubation with 3 different integrin inhibitors (BIO1211, BOP, TCS2314), particularly for cells treated with Lys679Met FXIII-A compared to WT FXIII-A. (c) Graph shows reduced cell proliferation rates following FXIII-A treatment (WT or Lys679Met) compared to control after incubation with the 3 integrin inhibitors at 48 hours. (d) Western blot shows reduction of Collagen I expression after 48-hour treatment with ILDT235_238AAAA FXIII-A. (e) Graph shows reduced cell proliferation rate after site-directed mutagenesis of ILDT motif of FXIII-A. These effects for (f) and (g) are common to the WT and Lys679Met FXIII-A but are more marked with Lys679Met FXIII-A. Experiments were performed in triplicate. The data show means \pm SD for three experiments * = $p < 0.05$ vs control ** = $p < 0.01$ vs control *** = $p < 0.001$ vs control. C, W and M indicates control, wild type or mutant, respectively.

1
2
3
4
5
6
7
8
9
10
11
12
13
14
15
16
17
18
19
20
21
22
23
24
25
26
27
28
29
30
31
32
33
34
35
36
37
38
39
40
41
42
43
44
45
46
47
48
49
50
51
52
53
54
55
56
57
58
59
60

167x274mm (300 x 300 DPI)

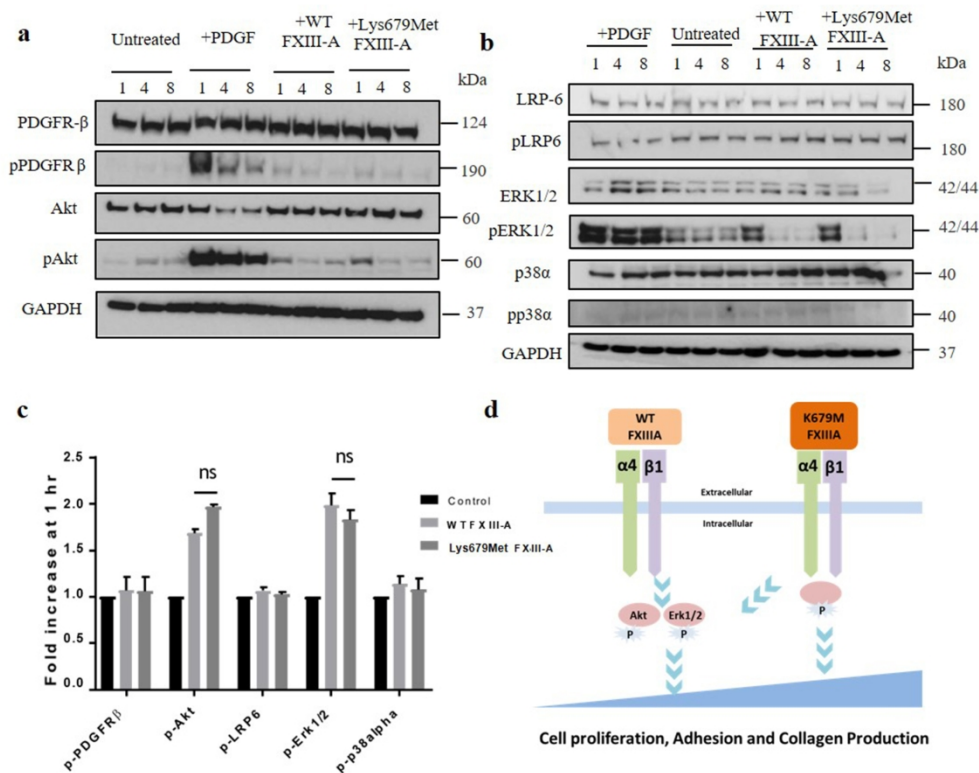


Figure 6: WT and Lys679Met FXIII-A both increase Akt and ERK1/2 activation. (a) NHDFs were treated with FXIII-A for 1, 4, or 8 hours with 2 nM PDGF-BB treatment as a positive control. Activation levels of PDGFR and Akt were determined by immunoblotting with antibodies to Tyr (p)-751-PDGFRβ and Ser(p)-473-Akt1. All samples were normalized for equal amount with glyceraldehyde-3-phosphate dehydrogenase (GAPDH). No activation was noted for p-PDGFR whereas both WT and Lys679Met FXIII-A showed transient increase in p-Akt signaling at 1 hour. (b) Activation level of LRP-6, ERK1/2 and p38α were determined by immunoblotting with antibodies to Ser (p)-1490-LRP6, Thr202 (p)/Thr204 (p)-p44/42MAPK (ERK1/2) and Thr (p)-180/Tyr (p)-182-p38α. All samples were normalized for equal amounts with GAPDH. Both WT and Lys679Met FXIII-A showed transient increase in p-ERK1/2 signaling at 1 hour. (c) Phosphoproteins were quantified, averaged and expressed for NHDF cells treated with WT and Lys679Met FXIII-A as fold change over those of untreated cells. Both WT and Lys679Met FXIII-A showed similar ~two-fold increases in p-Akt and p-ERK1/2 compared to control. Shown are the means +/- SD for three experiments. (d) A proposed schematic figure for FXIII-A and α4β1 integrins association on the cell surface and downstream signaling. Lys679Met may lead to a conformational change in the protein which promotes α4 integrin binding (right panel). WT and Lys679Met FXIII-A after association with integrins activate Akt and Erk1/2 resulting in cell proliferation, adhesion and collagen production. However, the enhanced action of mutant FXIII-A on α4 integrin could initiate different signaling cascades which still remain to be determined.

181x151mm (300 x 300 DPI)

1
2
3 **Supplementary information:**
4
5
6
7
8

9 **Coagulation Factor XIII-A Subunit Missense Mutation in the Pathobiology of Autosomal**
10 **Dominant Multiple Dermatofibromas**
11
12
13
14
15

16 Chavalit Supsrinunjai^{1,2}, Chao-Kai Hsu^{1,3,4}, Magdalene Michael⁵, Cédric Duval⁶, John Y. W.
17 Lee¹, Hsing-San Yang³, Hsin-Yu Huang⁷, Thitiwat Chaikul¹, Alexandros Onoufriadis¹,
18 Roberto Steiner³, Robert A. S. Ariëns⁴, Ofer Sarig⁸, Eli Sprecher^{8,9}, Marina Schwartz-Eskin⁸,
19 Roberto Steiner³, Robert A. S. Ariëns⁴, Ofer Sarig⁸, Eli Sprecher^{8,9}, Marina Schwartz-Eskin⁸,
20 Curt Samlaska¹⁰, Michael A. Simpson¹¹, Eduardo Calonje^{1, 12}, Maddy Parsons^{5*}, John A.
21 McGrath^{1*}
22
23
24
25
26
27
28
29
30
31
32
33
34
35
36
37
38
39
40
41
42
43
44
45
46
47
48
49
50
51
52
53
54
55
56
57
58
59
60

Table S1: A summary of the stepwise filtering approach to identify potentially shared variant within two pedigrees

Pedigrees	Family 1 (Ukraine)			Family 2 (USA)				
	I-2	II-2	III-1	II-1	II-3	II-2	III-2	II-5
Total variants	26063	26327	26278	26006	26072	26061	26236	25818
Variants with MAF<0.01 in 1000 genomes, ESP, ExAC and 6000 control exomes	1098	870	849	911	893	952	936	881
Heterozygous variants	768	850	833	872	866	918	910	852
Heterozygous nonsynonymous, splice-site, or insertion/deletion variants	556	541	526	530	496	578	808	530
Shared variants among affected individuals	118			113				
Genes with variants that are shared between the two pedigrees	1 (<i>FL3A1</i>)							

Table S2: A summary of the statistics of exome sequencing and coverage

Case	USA family					Ukraine family		
	II-1	II-3	II-2	III-2	II-5	I-2	II-2	III-1
Total reads	75853390	80748322	55446430	86094748	68319976	92053964	103018007	106717428
Reads uniquely mapped to +/- 150 bp of the target sequence	41705779 (54.98%)	43183922 (53.48%)	30637737 (55.26%)	47083150 (54.69%)	35757820 (52.34%)	71957989 (78.17%)	80224711 (77.87%)	83043872 (77.82%)
Reads uniquely mapped to target sequence	38934653 (51.33%)	40209995 (49.8%)	28501204 (51.4%)	43584762 (50.62%)	33379406 (48.86%)	65046797 (70.66%)	72451957 (70.33%)	74728981 (70.03%)
Mean_Coverage (reads per position)	81.49	82.54	58.58	90.98	67.89	122.86	136.85	140.54
Target CCDS bases	33323618	33323618	33323618	33323618	33323618	33323618	33323618	33323618
CCDS bases with coverage > 1x	33113976 (99.37%)	33109377 (99.36%)	33140600 (99.45%)	33147115 (99.47%)	33067174 (99.23%)	32979225 (98.97%)	33001727 (99.03%)	33003929 (99.04%)
CCDS bases with coverage > 5x	32754189 (98.29%)	32721647 (98.19%)	32734490 (98.23%)	32792592 (98.41%)	32528456 (97.61%)	32753490 (98.29%)	32795207 (98.41%)	32789252 (98.4%)
CCDS bases with coverage > 10x	32241535 (96.75%)	32181220 (96.57%)	31910596 (95.76%)	32289315 (96.9%)	31807387 (95.45%)	32513166 (97.57%)	32600284 (97.83%)	32581726 (97.77%)
CCDS bases with coverage > 20x	31106314 (93.35%)	31018109 (93.08%)	29043630 (87.16%)	31234256 (93.73%)	30095747 (90.31%)	31826135 (95.51%)	32059438 (96.21%)	32031001 (96.12%)

*CCDS: Consensus coding sequence

Supplementary Methods and Results

F13A1 analysis in sporadic, non-familial dermatofibromas

We performed Sanger sequencing on 22 Taiwanese sporadic dermatofibroma samples and 28 in-house sporadic dermatofibromas sample to determine whether Lys679Met variants and other potential variants are present in any sporadic dermatofibromas. We also hypothesized that variants in the promoter region of *F13A1* might be associated with sporadic dermatofibroma. In order to determine single nucleotide polymorphisms (SNPs) in this area, Sanger sequencing was performed on *F13A1* gene and its promoter region. Regarding promoter region sequencing, we divided the promoter region (2400 bases) into 5 segments overlapping each other. The length of each segment is approximately 500 bases. Forward and reverse primers for each segment were designed by using an online tool (Primer 3) resulted in 5 pairs of primers (Supplementary table S6). A total of 50 sporadic dermatofibroma were sequenced for *F13A1* gene and 22 DNA samples for promoter region. AmpliTaq Gold® 360 Master Mix (Thermofisher) and PCR protocol were used as previously described. The ABI 3730 DNA Sequencer (SeqGen, CA, USA) was then used for analyzing the sequence. The allele frequencies of each SNPs were compared with population databases, i.e. 1000 Genome Project and ExAC Browser, where available. For unreported SNPs, we compared with 30, in-house Taiwanese control samples. All 50 sporadic dermatofibroma were successfully sequenced for a further SNPs analysis. The total of 3 variants in *F13A1* and 5 variants in promoter region were identified from Sanger sequencing (Supplementary table S3 and S4). None of these variants was statistically significant and different from the variants in the population database as compared by using Hardy-Weinberg equilibrium calculation and chi-square test (GraphPad Prism® version 8).

Table S3: Hardy-Weinberg equilibrium and chi-square test for analysis of SNPs in *F13A1* from sporadic dermatofibromas

Variant	Homozygous variant		Heterozygous variant		Wild type		P value (two-tailed)
	Observed #	Expected #	Observed #	Expected #	Observed #	Expected #	
rs5982 (c.1694C>T)	3	4.67	18	21.09	27	22.24	0.3561
rs5987 (c.1951G>A)	0	0.4	6	8.62	42	38.98	0.4889
rs5988 (c.1954G>C)	0	0.41	7	8.69	41	38.89	0.6517

Table S4: Hardy-Weinberg equilibrium and chi-square test for analysis of SNPs in *F13A1* promoter region from sporadic dermatofibromas

Variant	Homozygous variant		Heterozygote		Homozygous reference		P value (two-tailed)
	Observed #	Expected #	Observed #	Expected #	Observed #	Expected #	
rs1024231	9	8.715	9	9.996	3	2.289	0.8481
rs2815822	21	18.84	0	2.121	0	0.042	0.2995
rs1016925	0	0.42	5	6.867	13.71	16	0.5197
rs1267856	0	2.06	8	8.84	12	9.1	0.2161
rs1267855	2	2.74	7	9.44	11	7.82	0.3458

Exon	Forward Sequence	T _m (°C)	Reverse Sequence	T _m (°C)
Exon 2	ACATGCCTTTTCTGTTGTCTTC	56.5	CTGGACCCAGAGTGGTG	57.6
Exon 3	CAACCCTGTTTTTCTTGTTTC	54.0	CAATGCAACCCATGGTGTC	56.7
Exon 4	GGCTTGTGAAATCAACCTAAC	55.9	GAAAATAAAATGTCTGCCTC	53.2
Exon 5	ACAGTCTGTTTGGTAATAG	53.2	GACAATAACAAATTTTAAGTGG	50.9
Exon 6	AGAGAATATTTTGCTTGCAGAG	54.7	GGCAAATGACAGGTGTAACAG	57.9
Exon 7	CCTTCTCACTTCTCACGGAC	59.4	AAGAAATTAAGTGGGATAC	52.8
Exon 8	GTGATGTGTTTAGCTGTGGT	55.3	GATTGAGTCTATCTTGTGGT	53.2
Exon 9	GGGATTACAGGCATGAGCCAC	61.8	AGATCAGCAATGAAGCAAGTCC	58.9
Exon 10	TGGACAGAATTGGGAGATGAC	57.9	TGTGTTAAGAGGTTGGGGAG	57.3
Exon 11	ATGATGGCTAATGCTCTCCT	55.3	TTCTCTGGAACCTCATCTCTG	55.3

Table S5 Primers for *F13A1*

Exon 12	CTGGTGGATTGTATTTTGCC	55.9	ACAGCGAGTCTCACAAAGAAC	57.9	
Exon 13	TGTGTGTGTTTTCTCCTACT	53.2	TTTGICTCTGTCCAGGATG	55.3	
Exon 14	AGAGCAGAACGAGGTTTTATTG	57.1	CACACAGAGAAAGCTTCCCAC	59.8	
Segment	position	Forward	Tm	Reverse	Tm
Exon 15	TCTCCGAA	ACCTCTCCTCTC	59.4	CCCCTGCAGTCCTGTCTGG	63.5
1	6:6321519 (-2678) – 6320920 (-2079)	GGCATGCACCTGTAGTTCC	59.1	AACCAGTTGCTGGGAGTACC	59.07
2	6:6321008 (-2344) – 6320456 (-1792)	AAACCCTCCCAGACCCTCT	59.9	GCAAGTGGAGCTGCCTGT	60.1
3	6:6320531 (-1867) – 6319949 (-1285)	ACCTCGGTTTCCTGGTTGA	60.5	TGAGAAATACCGAAGGTAGGC	58.3
4	6:6320031 (-1367) – 6319487 (-823)	CCCCTTAGCACTGTGTCTCC	59.7	GCAGGCACTGAGCCAGTTTA	61.5
5	6:6319570	CCCTTCATTTGGTCATTGG	60.2	TGCATGTGCTGTATCTATGTTCA	59.3

Table S6 Primers for *FI3A1* promoter region (6: 6,319,201 – 6,321,384:-1; 2 KB upstream from start codon of *FI3A1*)

	(-906) –				
	6319039				
	Forward (-375)		Tm (°C)	Reverse	Tm (°C)
Lys679	CCA ATG AAG ATG ATG TCC CGT	69.5	CAC GGT GGA GTT GGG CCG GAT TTC ACG	67.0	
Met	GAA ATC CGG CCC AAC TCC ACC		GGA CAT CAT CTT CAT TGG		
FXIII A	GTG				
FXIII A	CTC TGT CCA TCA CAT ACA GGC	93.5	AGC TAT GGT CAG TTT GAA GAT <u>GGC</u>	93.5	
with	AAG <u>CGG CCG CGG CGC</u> CAT		<u>GCC GCG GCC GCT</u> TGC CTG TAT GTG		
AAAA	CTT CAA ACT GAC CAT AGC T		ATG GAC AGA G		

Table S7 Primers for site directed mutagenesis

Antibody	Product no.	Manufacturer	Concentration	Application
Human Integrin alpha 4/CD49d MAb (Clone 7.2R)	MAB1354	bioTechne	1:100 IF 1:1000 WB	IF, WB
Mouse monoclonal [12G10] to Integrin beta 1	NB100-63255	bioTechne	1:100 IF	IF
Rabbit polyclonal to FXIII-A	ab97636	Abcam	1:1000	WB
Sheep polyclonal to FXIII-A	ab 104559	Abcam	1:100	IF
Mouse monoclonal to Collagen I	sc-293182	SantaCruz	1:200	WB
Mouse monoclonal to Collagen I	ab 90395	Abcam	1/2000	IF
Rabbit monoclonal [Y92] to PDGF Receptor beta	ab32570	Abcam	1:100 IF 1:5000 WB	IF, WB
Rabbit polyclonal to phosphor-PDGF-Receptor β (Tyr751)	3161	Cell Signaling Technology	1:1000	WB

Table S8 Primary and Secondary Antibodies

Polyclonal rabbit IgG to p38 α	AF8691	bioTechne	0.5 μ g/mL	WB
Mouse monoclonal to human phospho-p38 α	MAB8691	bioTechne	0.5 μ g/mL	WB
Rabbit polyclonal antibody to Akt	9272	Cell Signaling Technology	1:1000	WB
Antibody	Product no.	Manufacturer	Concentration	Application
Rabbit polyclonal antibody to pAkt(Ser473)	9271	Cell Signaling Technology	1:1000	WB
Rabbit IgG antibody to LRP-6	2560	Cell Signaling Technology	1:1000	WB
Rabbit polyclonal to phosphor-LRP6(Ser1490) antibody	2568	Cell Signaling Technology	1:1000	WB
Rabbit IgG antibody to p44/42 MAPK(ERK1/2) antibody	4695	Cell Signaling Technology	1:1000	WB
Rabbit IgG antibody to phosphor-p44/42 MAPK(ERK1/2)(Thr202/Tyr204) antibody	4370	Cell Signaling Technology	1:1000	WB

Rabbit polyclonal to fibronectin	ab2413	Abcam	1:100 IF 1:1000 WB	IF, WB
Rabbit polyclonal to GAPDH	ab9485	Abcam	1:2500	WB
Polyclonal Goat anti-rabbit Ig-HRP	P0448	Dako	1: 5000	WB
Polyclonal Goat anti-mouse Ig-HRP	P0447	Dako	1:2000	WB
Antibody	Product no.	Manufacturer	Concentration	Application
Mouse IgGκ binding protein-HRP	sc-516102	Santacruz	1: 1000	WB
Donkey Anti-Rabbit IgG H&L (Alexa Fluor 647)	ab150075	Abcam	1:200	IF
Donkey Anti-Sheep IgG H&L (Alexa Fluor; 568)	ab150177	Abcam	1:200	IF
Goat Anti-Mouse IgG H&L (Alexa Fluor 488)	ab150113	Abcam	1:200	IF

WB, western blot; IF, immunofluorescence; HRP, horseradish peroxidase

Supplementary Figures:

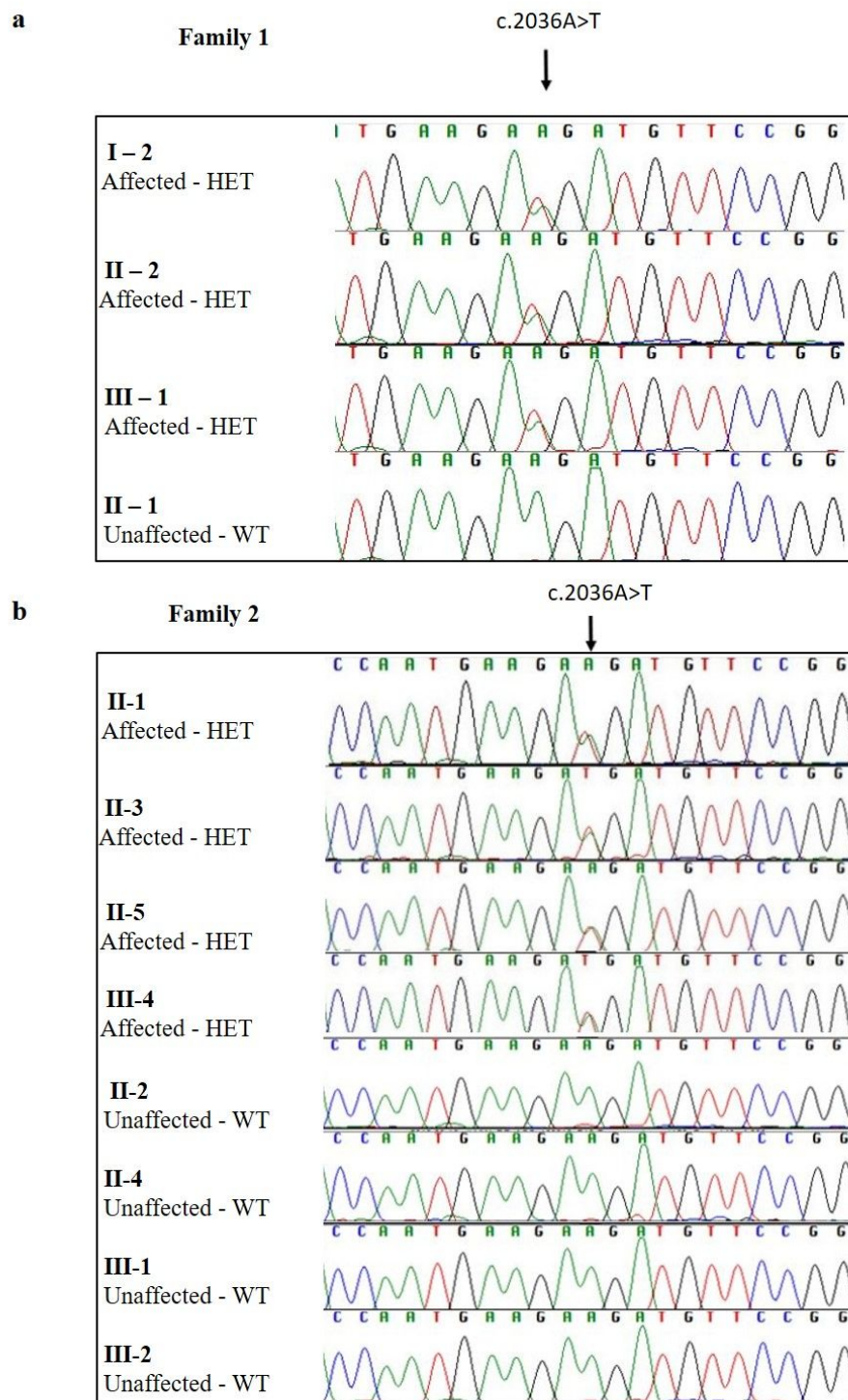


Figure S1. Chromatograms of *F13A1* gene reveals the heterozygous variant c.2036A>T (Lys679Met) in all affected subjects.

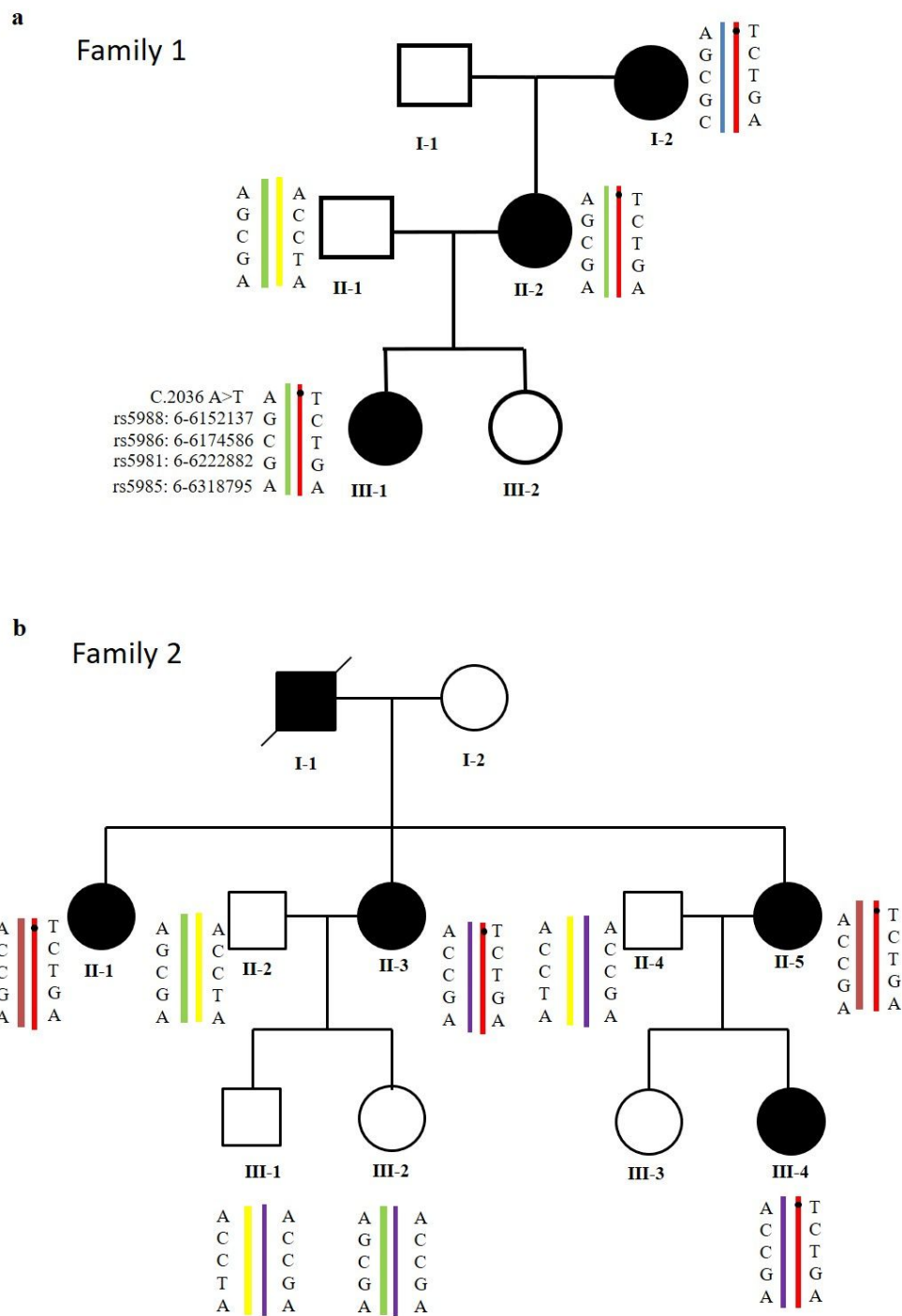


Figure S2. Haplotype analysis supports a common ancestral *F13A1* mutant allele in families 1 and 2. (a, b) SNP genotyping of two individuals in two families and their relatives with four highly polymorphic markers within *F13A1* shows that the individuals share the same haplogroup for the *F13A1* containing c.2036A>T (indicated by black spot). Each color bar represents a distinct haplotype.

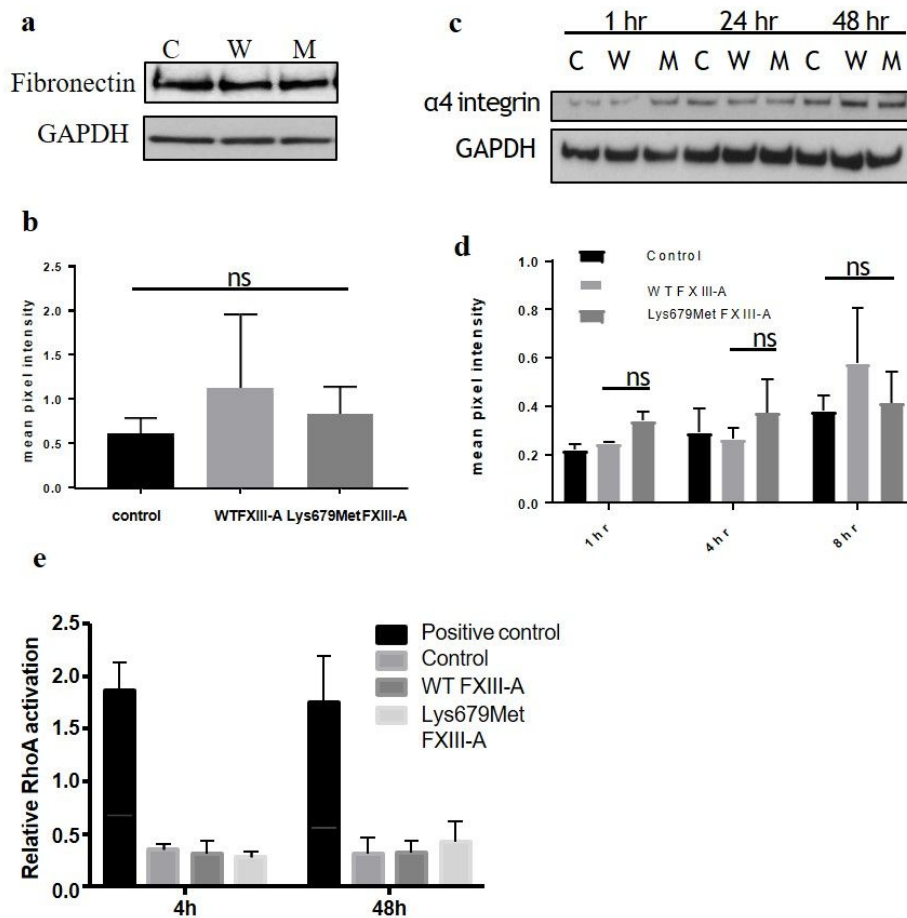


Figure S3: Levels of fibronectin and $\alpha 4$ integrin show no significant differences between treatments with either wild-type or mutant FXIII. (a, b) NHDFs were treated with FXIII for 48 hours with WT and Lys679Met FXIII; level of fibronectin was determined by immunoblotting with antibodies to Fibronectin. (c, d) NHDFs were treated with FXIII for 1, 24, 48 hours with WT and Lys679Met FXIII; level of $\alpha 4$ integrin was determined by immunoblotting. All samples were normalized for equal amounts with GAPDH. (e) NHDFs were treated with FXIII for 4 and 48 hours; level of RhoA was determined by GTPase-enzyme linked immunoabsorbent assay (G-LISA) Activation assays protocol (Cytoskeleton, Denver, CO). Shown are the means \pm SD for three experiments.